UNIVERSITY OF OKLAHOMA

GRADUATE COLLEGE

PALYNOLOGY OF THE UPPER FLOWERPOT FORMATION, MANGUM AREA, SOUTHWESTERN OKLAHOMA

A THESIS

SUBMITTED TO THE GRADUATE FACULTY

In partial fulfillment of the requirements for the

Degree of

MASTER OF SCIENCE

By

RYAN TOTTEN

Norman, Oklahoma

2022

PALYNOLOGY OF THE UPPER FLOWERPOT FORMATION, MANGUM AREA, SOUTHWESTERN OKLAHOMA

A THESIS APPROVED FOR THE

SCHOOL OF GEOSCIENCES

BY THE COMMITTEE CONSISTING OF

Dr. Richard Lupia, Chair

Dr. Stephen Westrop

Dr. Michael Soreghan

ACKNOWLEDGMENTS

I would like to thank first and foremost, Dr. Richard Lupia, for his infinite patience, enduring support, invaluable contributions, and insightful suggestions without which my thesis would not have been completed. I am forever indebted and grateful for his mentorship and friendship.

I would also like to thank my other committee members, Dr. Stephen Westrop and Dr. Michael Soreghan, for their help and encouragement during my research. Without Dr. Westrop's advice, I would not have pursued and completed this graduate degree.

There are numerous other people who have also made important impressions and lasting positive influences throughout my time here at the University of Oklahoma: Dr. Lynn Soreghan, Dr. Shannon Dulin, Rebecca Fay, Dr. Michael Engel, and Dr. Neil Suneson.

Lastly, I would like to thank Dr. Kenneth Johnson. His prolific work and publications in the geological literature formed the reference for much of my research. His passion for geology has been an inspiration to me.

From a personal perspective, I would like to thank my mother who was a constant source of positivity, encouragement, and support, not only for my time during my research, but throughout my life. I wouldn't have made it this far without her help. And to my girlfriend, Leslie Milam, who endured the vicissitudes of graduate school with me and was unwavering in her support. Besides myself, there is no one more pleased that my thesis is complete. And to my grandparents Melvin and Wincie, and my aunt Joyce, who are no longer with us, I know they would be proud. BOOMER SOONER!!!

TABLE OF CONTENTS

ABSTRACT

My study examines the plant palynomorphs recovered from a new section of the uppermost Flowerpot Formation of middle Permian age in southwestern Oklahoma. My goal is to document the species diversity and abundance of plant taxa using palynology—dispersed pollen and spores—and to compare observations with prior studies from leaves and palynomorphs, during an interval of time near the end of the Late Paleozoic Ice Age. Based on correlative megafossils in adjacent areas, this interval marks a profound expansion of seed plants and of a seasonally dry/arid climate in the region. My results are in agreement with these general patterns. Although showing relatively equivalent diversity of pollen (e.g., from seed plants) and spores (e.g., from ferns), my samples illustrate an overwhelming abundance of striate bisaccate pollen, in particular of the genus *Lueckisporites*, indicative of dry climate, and low abundance of free-sporing plants (e.g., mosses, ferns). In my sampled section, a conspicuous layer of copper bearing minerals was observed. Three samples were tested using x-ray fluorescence and registered markedly high concentrations of copper. The prevalence of palynomorphs in the upper Flowerpot Formation in southwestern Oklahoma, widely noted by previous investigators, might be related to the stratigraphic and diagenetic conditions that also foster copper deposition, but this requires further investigation.

INTRODUCTION

The rock record of the late Paleozoic in western equatorial Pangea preserves the transition from the ever-wet, coal-forming environments of the Carboniferous to warmer and more arid conditions of the Permian. This rock record must not be read literally due to taphonomic and sampling (mega)biases (DiMichele et al., 2020), but nevertheless captures the overall climatological transition in Oklahoma as North America drifted northward, higher into the drier midlatitudes (Montanez and Poulson, 2013) and the Late Paleozoic Ice Age (LPIA) came to an end (Montanez et al., 2007).

The polar ice caps of the Late Paleozoic Ice Age formed as Gondwana moved over the southern polar region during the latest Devonian and ushered the Earth into icehouse conditions that lasted through the early Permian (Lakin et al., 2016). Pangea also had mostly reached is full assembly during the early Permian. The subsequent deglaciation shifted the Earth into a greenhouse state that would last until the late Cenozoic (Scotese and Langford, 1995; Crowell, 1995). The tectonic and glacial/interglacial cycles had a significant impact on the climatic patterns and sea levels of the late Paleozoic that in turn greatly influenced the structure of the plant biota in equatorial Pangea (Gastaldo et al., 1996). These changes are documented in the floral landscape of the area showing the oscillation between, and ultimate transition from more hydrophilous plants typical of peat swamps (e.g., spore-producing plants, like lycopsids and ferns) to more xeromorphic plants (e.g., conifers, cycads) typical of drier environments that would come to prevail across the landscape as glaciation ended by the late Permian (DiMichele et al., 2001).

The Permian Period marks the only fossil record we have of a vegetational transition occurring at the end of a prolonged glacial period (Montanez and Poulson, 2013). Thus this interval is of crucial importance for understanding patterns, processes, and rates of change

analogous to present and future climate changes in the Holocene/"Anthropocene". My study looked at the palynology of the upper Flowerpot Formation that is roughly constrained to near the Leonardian–Guadalupian (Kungurian–Roadian) boundary and its record of the vegetation near the end of the LPIA. Previous studies of the vegetation of the Flowerpot Formation by Wilson (1962), Morgan (1967) and Clapham (1970) reached variable conclusions. Wilson (and Morgan) concluded that the Flowerpot Formation was a marine deposit in dry climate, while Clapham found spore-rich horizons that he concluded represented episodic expansions of wetter habitats locally. The goals of my investigation were to analyze the palynology from a previously unstudied outcrop nearly 10 km distant from any prior sample site, but from a correlative stratigraphic interval, to test the hypothesis that spatial variation is sufficient to explain the disparate conclusions, and to support or refute the marine deposit hypothesis of Wilson (1962). In addition, while prospecting for this site, I encountered copper, in the form of malachite, weathering out of the targeted stratigraphic interval. Based on studies of the Creta Copper Mine (Hagni and Gann, in Johnson and Croy, 1976) that showed preserved spores from the productive copper beds, my study aimed to begin the investigation of the relationship between palynological (pollen and spore) recovery in samples with the abundance of copper in the sediments.

LATE PALEOZOIC: GLOBAL PALEOGEOGRAPHY and PALEOCLIMATE

Permian strata in western equatorial Pangaea are characterized by thick sequences of clastic red beds and evaporites giving the impression of the era as hot, dry, and desert-like (Clapham, 1970). However, on a finer temporal scale, evidence shows a more complex picture of the Permian landscape that had its origins in the late Devonian. (Isbell et al., 2008).

During the late Devonian, a large portion of Gondwana was positioned over the southern polar region (Figure 1) (Scotese et al., 1985). A drawdown of CO_2, attributed in part to an

expanse and sequestration of peat swamps in paleotropical regions, contributed to overall cooling of the Earth and formation of continental glaciers in Gondwana, ushering the world into icehouse conditions (Montanez et al., 2007; Chaloner and McElwain, 1997). As Gondwana drifted north and began colliding with Laurussia around the mid-Carboniferous boundary (Blakey, 2008), equatorial oceanic currents were disrupted that, in turn, influenced atmospheric circulation deflecting heat and vapor poleward intensifying the growth of continental ice sheets in southern Gondwana (Saltzman, 2003; Montanez and Poulson, 2013). In addition, equatorial tectonic uplift caused by the evolution of Pangaea also may have contributed to lower CO_2 levels by increasing silicate weathering (Godderis et al., 2017; Berner, 2018). Although there is no single "smoking gun" that caused the LPIA, the combination of forcings and feedbacks—including orbital cycles, oceanic and atmospheric circulation patterns, floral expansion and burial, tectonics in the form of volcanic aerosols (Soreghan et al., 2019), and continental positioning—all contributed to the creation of continental glaciers in Gondwana.

Details of global Late Paleozoic glaciation patterns are still debated, but there is general consensus on three major glaciated intervals: late Devonian/Tournasian (~365–345 Ma); late Visean into the Bashkirian (~335–320 Ma; mid-Carboniferous boundary); and Asselian/Artinskian (299–280 Ma) (Isbell et al., 2003; Montanez et al., 2007). Furthermore, recent evidence suggests these intervals had multiple ice sheets originating from multiple ice centers in the southern parts of Gondwana (Montanez and Poulsen, 2013). It is also important to consider there were numerous glacial/interglacial cycles within these broad glaciated intervals. The advance and retreat of these glaciers during the late Paleozoic continued into the Permian and caused sea level fluctuations estimated between 50–150 m (Montanez and Poulson, 2013). Far-field sedimentological evidence in the form of cyclothems is inferred for these fluctuations

in sea level found throughout the world (Heckel et al., 2007). Cyclothems are units of strata usually, but not always, comprised of marine and terrestrial elements reflecting cyclic oscillations of sea level and climate (DiMichele et al., 2020). Most fully developed in areas that were broad and flat over a large area, idealized cyclothems of a transgressive phase would be composed of fluvio-deltaic deposits followed by peat/coal formations continuing up through a shallow marine limestone and finally a deep marine 'core shale' (Wicander and Monroe, 2013). Idealized cyclothems are separated by an erosional surface.

By the early Permian, glaciation had reached its peak (Montanez and Poulson, 2013), formation of the Pangean supercontinent was essentially complete, and significant tectonic activity decreased (Stampfli et al., 2013). The formation of Pangaea created an enormous mountain chain, collectively referred to as the Central Pangean Mountains, located near the paleoequator (Wicander and Monroe, 2013). The effects of continentality increased across the interiors of the continent and the deposition of red beds and evaporites became more prevalent (Ziegler et al., 2002). In addition, as Pangea continued to drift north, equatorial zonal circulation patterns were disrupted leading to more pronounced monsoonal effects of increased seasonality (Parrish, 1995). In fact, these effects led to the demise of glaciation and ushered the world into greenhouse conditions. Cumulatively, the Late Devonian through Early Permian contains the only fossil record recording the entry and exit of a vegetated Earth from an ice age (Montanez and Poulson, 2013).

LATE PALEOZOIC: MID-CONTINENT PALEOCLIMATE and PALEOBOTANY

In view of the uniqueness of the Early-to-Late Permian fossil record in recording the transition from an "Ice House" to "Greenhouse" climate state, the exploration and documentation of localized climate and vegetation patterns during this period has tremendous

relevance for informing our understanding and expectations regarding the analogous climate shift we are experiencing now in the Pleistocene to Holocene to Anthropocene(?) transition.

The long-term trend from the Carboniferous through the Permian was certainly leading to warmer and drier conditions, but local microenvironments indicate a more heterogenous landscape and show the oscillations and co-occurrence of plants with wetter affinities existing near those with drier affinities. For instance, during the Pennsylvanian, much of the North American study area was equatorial with estimates for Oklahoma and Kansas ranging from 0–5° N latitude and those from Texas and New Mexico from +/- 5° N or S (Golonka and Ford, 2000). Ever-wet climatic conditions and hypoxic soil conditions were prevalent and significant portions of Texas, Oklahoma, Kansas, Alabama, and Illinois, as well as numerous locations worldwide, collectively referred to as the Euramerican equatorial coal belt, produced Pennsylvanian age coal beds (DiMichele et al., 2001). These famous Euramerican coal beds began developing in the latest Mississippian and continued intermittently into the Middle Pennsylvanian in response to the onset of glaciation (Raymond, 1996; DiMichele et al., 2001).

Macrofossil floral data from various regions around the North American mid-continent demonstrates the transition from the more wet conditions of the Pennsylvanian to the increasingly drier, more arid conditions characteristic of the Permian. This tropical coal belt can be simplistically divided into two provinces: wetlands (ever wet) and seasonally dry (mostly wet) (DiMichele, 2014). Peat swamps formed in the wetlands and evidence from coal balls (Phillips et al., 1976) indicate tree forming lycopods and giant club mosses, both spore producers, were the dominant vegetation. Lycopods, which have a greater affinity for wetter substrates, dominate the peat fossil record for lower to middle Pennsylvanian but rather abruptly give way in the upper Pennsylvanian to marattialean tree ferns and primitive seed plants whose ecological affinities are

both more tolerant of dry periods than lycopods (Pfefferkorn and Thomson, 1982). It is important to note that plant assemblages forming in the upland areas of the basin during this time interval tend to be more frequently dominated by seed plants than their wetland counterparts dominated by spore-producers (DiMichele et al., 2001, but see DiMichele et al. 2020 or megabias effect on this simple interpretation). When climatic influences are favorable—e.g., short global warming periods and/or glacial/interglacial pulses, these seed plants (such as conifers, pteridosperms, ginkgophytes, and cycads) that are much more adapted to drier environments than lycopods invade the wetland biomes and come to dominate the fossil record during the Permian (Looy et al., 2014).

Specific examples from around the North American paleocontinent basins (including from beyond the mid-continent proper) illustrate the distribution of plant macrofossils during the Late Paleozoic. Chronologically, the Pottsville Formation from the Black Warrior Basin in Alabama is late Carboniferous (Bashkirian; ~315 Ma) in age (Pfefferkorn et al., 2008). Macrofloral fossils from the lower part of the formation show the strata dominated by lycopods, sphenopsid (horse tails), and cordaitalean canopy trees (primitive conifers) (Pfefferkorn et al., 2008). Within the Pottsville Formation, four distinct coal seams are evident and in situ forests are preserved showing an abundance of lepidodendrids and sigillarians, both of which are lycopods (Pfefferkorn et al., 2008).

The Brazil Formation of the Illinois Basin in southwest Indiana is late Carboniferous (Moscovian; ~310 Ma) in age and demonstrates a macrofossil assemblage similar to the Black Warrior Basin. Most of the major groups of Carboniferous plants are represented: lycopods, tree ferns, sphenopsids, and cordaites (DiMichele and Beall, 1990). The younger Carbondale Formation in the Illinois Basin, which is also Moscovian (~308 Ma), shows repetitive sequences

of marine and terrestrial cyclothems (Pfefferkorn et al., 2008). Within these cyclothems, are numerous coal beds that provide supporting insight into the floral make-up of this time interval. Lycopods dominate most of the plant assemblages up to near the Westphalian-Stephanian (Kasimovian–Gzhelian) boundary when they abruptly decrease in abundance and are replaced by a dramatically increased abundance of tree ferns in the Stephanian (Figure 2) (Pfefferkorn et al., 2008).

The Markley Formation of north-Central Texas is roughly constrained to the Permian-Carboniferous boundary interval (~299 Ma) and plant macrofossils are found in discrete horizons falling into two broad categories based on lithology and depositional environments. Shales and floodplain deposits are dominated by one taxon, medullosan pteridosperms, or if slightly less clastic, lycopods (DiMichele et al., 2005). In the second mudstone facies, periodically altered by pedogenesis, the flora is dominated by walchian conifers and the pteridosperm *Sphenopteridium*—both of which are associated with drier substrates. The variation of plant assemblages in the same formation is interpreted to represent climatic fluctuations in response glacial and interglacial cycles (DiMichele et al., 2005; Looy et al., 2014).

Plant megafossils from the Abo Formation of New Mexico also continues the pattern of increasing aridity in western equatorial Pangea during the Permian. Poorly constrained due to limited and sporadic exposures, the Abo Formation is generally accepted to Wolfcampian (Asselian–Artinskian) in age, ~299–280 Ma. This formation is dominated by conifers and supaioid and callipterid peltasperms (another seed plant clade), all of which are inferred to demonstrate seasonally dry affinities (DiMichele et al., 2013). Twenty-seven species of walchian conifers and peltasperms were found in the vast area of Abo Formation redbeds (DiMichele et al., 2007). In minor amounts, pteridosperms, sphenopsids, calamitalean stems, and marattialean

tree ferns were also discovered indicating a wetter environment locally. Macrofossils from the Hueco Group of New Mexico have been found in the Community Pit Formation also of lower Permian age. Interpreted to be coastal in origin, the autochthonous macrofloras are found in limestone channel fill and include voltzian conifers, and the callipterid, *Lodevia oxydata*, both pollen/seed producers (DiMichele et al., 2015).

Macrofloras from the Clear Fork Group of Leonardian (Artinskian–Kungurian; ~280–270 Ma) age of north central Texas continue the trend of a diverse but drying landscape. The first samples from cores through the Clear Fork Group are interpreted to record coastal settings, ranging from shallow subtidal, open marine environments in the lower part of the core to a "complex of shallow lagoons, shoals, tidal flats, beaches, and vegetated islands" in the upper part (DiMichele et al., 2000). The most abundant taxa represented in the cores are plants with a dry soil affinity, like the pteridosperm *Comia*, the cycad *Taeniopteris*, and the peltasperm *Delnortea abbotiae*. Another megaflora from the Clear Fork Group was identified in an outcrop interpreted to be channel-form deposits of mostly red silt and fine-to-medium sand. Thin layers of gypsum begin to appear in the middle of the group becoming more abundant toward the top demonstrating increasing climatic pulses of lower rainfall and higher evaporation. The Clear Fork Group is dominated by multiple species of seed plants with minor occurrences of tree ferns and other hydrophilous plants like ferns and horsetails. Even though these wetter affinity plants are rare, they persist in the assemblages at lower diversity going up-section (DiMichele et al., 2000).

Finally, overlying the Clear Fork Group is the Pease River Group (Guadalupian; Roadian–Capitanian; ~270–263 Ma), which contains one of the youngest Permian fossil floras yet identified in North America. The plant megafossils from the lower Pease River Group are

interpreted to have been deposited in "channel facies that originated as tidal channels within a coastal plain setting on the Eastern Shelf of the Midland Basin" (DiMichele et al., 2001, p. 449). The dominant megafossils comprise members of Coniferales, Ginkgoales, and Cycadales (DiMichele et al., 2001), which have dry/arid tolerances, and remnant Equisetales and Cordaitales that tend to favor wet habitats.

Studies employing palynological—spore and pollen—data are numerous from Pennsylvanian formations, but diminish through the section, becoming sporadic and spatially restricted in coverage from later Permian sediments. Nevertheless, palynological data from the region also demonstrate the transition from wetter conditions of the Carboniferous to the drier conditions of the Permian. Palynological data from the Lost Branch Formation and overlying Hepler Unit in Kansas illustrate the loss of lycopod-dominated assemblages and the transition to the seed fern and tree fern-dominated swamps just below the Moscovian–Kasimovian boundary (Peppers, 1997).

Lupia and Armitage (2013) used palynological samples from cores in northern Oklahoma to demonstrate the large-scale vegetational change during the latest Pennsylvanian (Virgilian; Gzhelian; ~300 Ma) into the early Permian (Leonardian; Kungurian; ~275 Ma). Although the long-term pattern of increasing aridity is maintained, there are more subtle differences in the palynofloras that reflect local and regional differences as well as the more frequent oscillations of glacial/interglacial cycles. While no noticeable floral change occurs across the Permian-Carboniferous boundary, by the Leonardian marked changes are apparent. Figure 4 illustrates the percentage abundance of various pollen and spores found in the cores spanning the Virgilian–Leonardian interval (Gzhelian–Kungurian; ~300 to ~275 Ma). Apparent are the considerable decrease in trilete and monolete spores from the latest Carboniferous, where they account for

well over 50% of the total count in samples, to Leonardian samples, where they are virtually absent. Monolete and trilete spores, whose ecological affinities are with wetter environments, are associated with ferns, horsetails, lycopsids, and tree ferns. Conversely, *Vittatina* and *Hamiapollenites*, whose ecological affinities are aligned more with dry environments, are seldom encountered in samples older than Leonardian but make up as much as 40% of the Leonardian sample count (Lupia and Armitage, 2013). This is consistent with the pattern of increasing aridity/dryness that has been discussed.

In summation, basinal plants during the coal-forming swamps of the Carboniferous were dominated by spore-producing plants and to a lesser extent, the extrabasinal and more derived primitive seed plants. Over time, with increasing fluctuations between aridity and wetness, these seed plant species would become established in basinal environments, with the concomitant decline in hydrophilous plant populations.

FLOWERPOT FORMATION: GEOLOGY and PALEOENVIRONMENT

The Flowerpot Formation was named by Cragin (1896) for layers of gypsiferous shale between the underlying Cedar Hills Sandstone the overlying Medicine Lodge Gypsum near its type locality at Flowerpot Mound in Barber County, Kansas (Fay, 1964). The areal exposure of the Flowerpot Formation runs from southwestern Kansas, from its type locality near Medicine Lodge, Kansas, through western Oklahoma and into north central Texas. At its type locality, the Flowerpot Formation thickness is 58 m. As it is traced southward into western Oklahoma, the Flowerpot reaches a maximum thickness of 142 m and interfingers with an inferred deltaic tongue of the Duncan Sandstone or its equivalent, the Chickasha Sandstone (Fay, 1964) and abruptly turns west-northwest along the northern side of the Wichita Mountains. In this area, the Flowerpot is overlain by the Haystack Gypsum, the lowermost member of the Blaine Formation

(Johnson, 1990). The formation then curls sharply south around the western surface exposure of the Wichita Mountains and is traced southward into the Hollis-Hardeman Basin of southwestern Oklahoma where the formation is ~61 m thick (Johnson, 1990) and finally into north-central Texas where the formation becomes the Flowerpot Member of the San Angelo Formation (Smith, 1974).

The Flowerpot Formation is upper Leonardian to lower Guadalupian (Kungurian–Roadian) in age (Johnson, 2021) and, in Oklahoma, is a part of the El Reno Group that includes in ascending order: Duncan Sandstone, Flowerpot Shale, Blaine Formation, and Dog Creek Shale (Johnson, 1989). In Kansas, the Flowerpot Formation is part of the Nippewalla Group (Benison and Goldstein, 2001), and in Texas, it is a member within the San Angelo Formation (Smith, 1974). The base of the Blaine Formation, the Haystack Gypsum member (also called Medicine Lodge member), forms a resistant impediment to erosion of the uppermost Flowerpot Formation and, along with other thick gypsums, serves as a strong correlative landmark across surface exposures in northwestern and southwestern Oklahoma known as the Blaine Escarpment (Sweet et al., 2013).

The area of study includes the uppermost 12 meters of the Flowerpot Formation of southwestern Oklahoma. During Leonardian time, the Flowerpot Formation occupied a paleogeographic position in western equatorial Pangea. Specifically, in my area the Flowerpot Formation is located on a regional high between the Hollis-Hardeman basin, which is considered the eastern edge of the Palo Duro Basin, and the Anadarko Basin. Although not as deep as the Anadarko Basin where the thickest portion of the Flowerpot Formation is exposed, the genesis and evolution of the Hollis-Hardeman Basin is related to the numerous highlands related to Pangaean suturing and associated uplifts. As Gondwana moved north from the southern polar

region, it rotated clockwise and began suturing the continents (Gondwana and Laurasia) together from the northeast to southwest in a series of orogenic events culminating in the Ouachita-Marathon orogeny (Gilbert, 1992). Even though the location of the Anadarko and Hollis-Hardeman basins was interior to the continental margin, far field stresses related to the compression of the Ouachita-Marathon orogeny significantly affected area, which was well into the cratonic interior. Uplift occurred as far north as the Ancestral Rocky Mountains, which was coincidental with the Wichita-Amarillo uplift (Kluth and Coney, 1981). Activity along the Wichita uplift had ceased by early Permian time, however, the basinal areas continued to subside well into the Permian but at much slower rate compared to the Pennsylvanian (Gilbert, 1992; Johnson, 1989). As much as 2 km of Permian sediments were deposited in the Anadarko Basin during the Permian (Johnson, 1989). Clastic input from the Wichita Mountains waned as the highlands were eventually buried by detritus (Johnson, 1989) and more clastic input originating from the Ouachita, Ozark, and/or Appalachian Mountains to the east, and/or Ancestral Rocky Mountains to the west (Fay, 1964; Gilbert, 1992; Sweet et al., 2013).

Based upon the abundance of fine grained clastics and evaporite rocks like dolomite and gypsum, the Flowerpot Formation formed in an arid to semi-arid, restricted coastal marine environment where evaporation rates exceeded rainfall rates. Periodic inundation of a shallow sea recharged the area and supplied fresh elements to form the evaporative sequences found in the El Reno Group. Conventional interpretations of the Permian red beds and accompanying evaporites, including gypsum and halite, usually invoke marine or marginal marine environment (Wilson, 1962) but other more recent analyses indicate a strong aeolian component and continental deposition (Benison and Goldstein, 2001; Giles et al., 2013; Sweet et al., 2013).

FLOWERPOT FORMATION: PREVIOUS PALYNOLOGICAL STUDIES

Despite extensive study, there are no published macrofossils localities from the Flowerpot. In contrast, several publications document numerous productive palynological—fossil pollen and spores—sites throughout the outcrop area in southwest (Wilson, 1962; Morgan, 1967; Clapham, 1970) and northwest Oklahoma (Clapham, 1970).

Permian fossil spores of the Flowerpot Formation were first described in southwestern Oklahoma in Greer County by Wilson (1962). Wilson's sample (Oklahoma Palynology Collection number 1 = OPC 1) was collected in an olive gray shale 30 feet below base of the Blaine Formation in NE ¼ SE ¼ SE ¼ sec 2, T4 N, R. 23 W (34° 50' 39.81" N, 99° 34' 42.50" W) about 8.5 km west-northwest of the current study site (Figure 5). Wilson's (1962) results show about 86% of 2000 counted specimens were saccate pollen, of which *Lueckisporites* comprised nearly 80%. All sacci-bearing pollen bear similarities to modern conifer species and Clement-Westerhof (1974) found *Lueckisporites* pollen directly associated with fossil cones of a plant with coniferalean affinity. Although most of the pollen is associated with upland conifer-like flora, the abundance of spores must be considered as well. Wilson (1962) postulated a paleoecology for the Flowerpot Formation described as:

> "(1) a shallow coastal marine or brackish water environment containing a restricted marine fauna, (2) an adjacent narrow zone of coastal swamp or an inlet containing swamp vegetation, and (3) a low upland or plain with a varied forest of conifers and other semi-arid plants, all characteristics of a warm temperate or subtropical climate" (Wilson, 1962, p. 33).

Regarding the restricted marine fauna, Wilson cites the examples of several specimens of one hystrichosphaerid species and one scolecodont fossil in the assemblage.

Subsequently, Morgan in an unpublished PhD dissertation (1967), sampled three cores at various horizons for palynological samples in the El Reno Group, comprised of the Flowerpot, Blaine and Dog Creek Shale formations. The first core was from Harmon County and consisted of productive palynological samples at several horizons in the Dog Creek Shale and Blaine Formations only. The second core from Blaine County yielded one palynological sample from the uppermost Flowerpot Formation. A third core (OPC 1072) from Greer County about 9 km west-southwest of the current study site in SW ¼ sec. 14, T 4 N, R 23 W (34° 48' 58.85" N, 99° 35' 37.42" W) contained four productive samples, three of which were in the upper Flowerpot. Of these three productive horizons, two were immediately above and below the Kiser Gypsum member and stratigraphically most equivalent to my current study site and of that of Wilson (1962). It is of note to mention that no gypsum bed equivalent to the Kiser Gypsum is reported at Wilson's site (Wilson, 1962). Morgan states that the sample from 138 ft depth in the core (locality OPC 1072), above the Kiser Gypsum, is the horizon most equivalent to Wilson's sample horizon. My current study site is more nearly stratigraphically equivalent to Morgan's sample from 154 ft depth in the core (OPC 1072). Morgan showed similar results to Wilson in the abundance of saccate pollen making up over 75% of the microfossils present. *Lueckisporites* sp. was again the dominant genus over the entire group of samples.

Clapham (1970) studied 62 palynologically productive horizons (out of 311 samples) in the upper Flowerpot Formation covering seven counties in Oklahoma. The samples are clustered and categorized into two areas defined by Clapham as the northeastern study area and the southwestern study area. Some of the samples from within the southwestern study are within 8 km of the current study site and also those of Wilson and Morgan. All samples from Clapham were within the top 10-35 feet of the Flowerpot. Furthermore, Clapham categorized the

assemblages into two groups, one considered the typical upper Permian flora dominated by *Lueckisporites,* and the other dominated by spore taxa, including *Psophosphaera* and *Paludospora,* that are associated with regressive intervals where coastal margins expanded. Clapham posits two floral assemblages of the upper Flowerpot time as "broad coastal salt marshes or swamps of regressive interval that were composed of ferns, cycadophytes, and conifers" (Clapham, 1970, p. 168) represented by the assemblages found in the cryptogamous category and "farther inland was an extensive, low, drained upland, populated mainly by conifers." (Clapham, 1970, p. 168) (Figures 6 and 7).

FLOWERPOT FORMATION: APPEARANCE OF COPPER

Copper deposits are well-known worldwide in association with Permian red bed deposits. The most famous and economically productive being the Kupferscheifer deposit in Germany that is still actively mined today (Sun and Puttmann, 2000). These stratiform copper deposits (as opposed to igneous copper deposits) are found throughout the world in lithological facies associated paralic marginal marine (or lacustrine) environments where red beds, evaporites, and reduced strata (often dark mudstones) are common (Cox et al., 2007).

The exact mechanisms for the stratiform copper deposits are debated but certain parameters for its deposition are widely accepted and may provide insight into the paleoenvironment of the middle Permian in my area. Stratiform copper deposits require four conditions to be present before formation (Cox et al., 2007). The first is the presence of oxidized red beds containing ferromagnesian minerals from which copper can be leached. Secondly, a brine source, provided by evaporitic environments in the form of hypersaline fluids, is needed to mobilize the copper (Davidson, 1965). Thirdly, a reduced fluid containing sulfide to catalyze the precipitation of the copper in the host sediment. Sulfide is produced as a by-product of bacterial

metabolism of organic material. Lastly, a permeable pre-lithified rock source must be present to provide adequate fluid mixing and pore space or bedding planes for deposition (Cox et al., 2007; Haynes, 1986).

In recent history, the Creta copper deposit in far southwestern Oklahoma was also a productive copper site producing 1,000 tons of copper ore per day (Johnson and Croy, 1976), producing from two zones, the main/lower copper bed 10 feet below the Kiser Gypsum ("Pruitt Copper Bed") and the upper copper bed 5 feet below the Kiser ("Meadows Copper Bed"). Although economically viable copper deposits are rare, numerous authors (e.g., Fay, 2000) have noted the appearance of copper in Permian red beds in varying amounts in the southwestern United States including Kansas (Wellington Formation and Ninnescah Shale) (Ripley et al., 1980), Oklahoma (Flowerpot Formation and Wellington Formation) (Johnson, 1976), Texas (San Angelo-Flowerpot) (DiMichele, et al. 2001), and New Mexico (Abo Formation) (LaPoint, 1974). These copper deposits are initially recognized, in situ, as green encrustations along bedding planes as an oxidized form of copper carbonate, malachite, which has been weathered from the original copper sulfide mineral, chalcocite.

Microscopy work by Hagni and Gann (1976) on copper ores from the Creta mine noticed that many of the copper sulfide grains were rounded to ellipsoidal and subsequently determined the copper had replaced spores dispersed in the strata. In addition, DiMichele et al. (2001) noted the occurrence of copper in association with plant bearing horizons in Permian formations in north central Texas near the San Angelo Formation and Blaine contact, which is stratigraphically correlative to my current study site, approximately 130 km away.

MATERIALS AND METHODS

My area of study is an outcrop of the Flowerpot Formation in the SE ¼ NE ¼ sec. 15, T. 4 N., R. 22 W (34° 49’ 32.25” N, 99° 29’ 35.35” W) (Figures 8 and 9). I measured a section with a 1.5 m Jacob staff beginning on N1950 Rd about 200 m south of E1510 Rd to the east side of the outcrop. The measurements totaled just under 25 m to the top of the Haystack member of the Blaine Formation where the outcrop terminated. With permission of the landowner, the measured area continued up-section from Haystack member about 100 m to the southwest to include another 14 m of the Blaine Formation to a thin layer of dolomite where the outcrop terminated.

The stratigraphic section (0 cm) begins at the road with Bed 1 and ends with Bed 43 at the top of the section. “Height (cumul.)” is the cumulative height in section to top of specified bed. Samples analyzed, for copper and/or palynology, are listed according to their Oklahoma Paleobotany Collection locality number (OPC#) and sample heights above base are stated. All measurements are in centimeters.

BED	THICKNESS	HEIGHT (cumul.)	DESCRIPTION
1	85	85	Covered
2	90	175	Mudstone, reddish brown to chocolate brown, sharp upper contact
3	10	185	Mudstone, grayish brown, sharp upper contact
4	8	193	Gypsum, sharp upper contact
5	28	221	Mudstone, reddish brown, gypsiferous, olive green interval, sharp upper contact
6	1	222	Mudstone, greenish gray, sharp upper contact
7	8	230	Gypsum, sharp upper contact

8	10	240	Mudstone, greenish gray
9	375	615	Mudstone, reddish brown, gradational upper contact
10	45	660	Muddy gypsum, gypsum stringers, gradational upper contact
11	70	730	Mudstone, bluish gray, sharp upper contact
12	7	737	Gypsum, sharp upper contact
13	100	837	Mudstone, reddish brown, gradational upper contact
14	5	842	Mudstone, grayish blue, sharp upper contact
15	70	912	Gypsum [= CHANEY GYPSUM], covered upper contact
16	150	1062	Covered interval, terrace top
17	150	1212	Mudstone, reddish brown, relatively sharp upper contact
18	45	1257	Mudstone, gray, gradational upper contact
19	20	1277	Mudstone, medium brown, relatively sharp upper contact, small 1 mm gypsum stringer 1275-1277 cm **OPC 2227** (sample)
20	84	1361	Mudstone [=? MEADOWS COPPER BED], olive gray, sharp upper contact. Malachite present on surfaces, bright green when fresh (“copper interval” of text) 1277-1281 cm **OPC 2228** (sample) 1281-1284 cm **OPC 2229** (sample)

1284-1286 cm **OPC 2230** (sample)

1286-1288 cm **OPC 2231** (sample)

1288-1291 cm **OPC 2232** (sample)

1291-1295 cm **OPC 2233** (sample)

1296-1298 cm **OPC 2234** (sample)

1299-1302 cm **OPC 2235** (sample)

1302-1305 cm **OPC 2236** (sample)

1307-1309 cm **OPC 2237** (sample)

1309-1311 cm **OPC 2238** (sample)

1311-1313 cm **OPC 2239** (sample)

1314-1316 cm **OPC 2240** (sample)

1317-1319 cm **OPC 2241** (sample)

1319-1321 cm **OPC 2242** (sample)

1321-1323 cm **OPC 2243** (sample)

1323-1325 cm **OPC 2244** (sample)

1325-1327cm **OPC 2245** (sample)

1327-1329 cm **OPC 2246** (sample)

1329-1331 cm **OPC 2247** (sample)

1334-1336 cm **OPC 2248** (sample)

1339-1341 cm **OPC 2249** (sample)

1344-1346 cm **OPC 2250** (sample)

1351-1353 cm **OPC 2251** (sample)

1356-1358 cm **OPC 2252** (sample)

			1359-1361 cm **OPC 2253** (sample)
21	7	1368	Gypsiferous mudstone, medium brown, sharp and flat upper contact
22	3	1371	Mudstone, grayish olive green, sharp upper contact
23	8	1379	Mudstone, medium brown, sharp upper contact, very thin gypsum stringers
24	8	1387	Mudstone, grayish olive green, sharp upper contact
			1382-1387 cm **OPC 2254** (sample)
25	17	1404	Gypsum [= KISER GYPSUM], sharp upper contact
26	10	1414	Mudstone, olive gray, gradational upper contact
			1404-1409 cm **OPC 2255** (sample)
27	25	1439	Mudstone, grayish brown, gradational upper contact
28	12	1451	Mudstone, olive gray, sharp upper contact
29	38	1489	Covered interval
30	2	1491	Dolomite, gray
31	130	1621	Covered interval
32	5	1626	Gypsum
33	250	1876	Mudstone, reddish brown, gradational upper contact
34	2	1896	Gypsum bed, sharp upper contact
35	150	2046	Mudstone, reddish brown, sharp upper contact
36	25	2071	Gypsum at base, alternately colored gypsiferous mudstone, wavy bedded

37	135	2206	Mudstone, gypsiferous, mottled gray/brown, wavy bedded
38	150	2356	Mudstone, gray
39	150	2506	Gypsum [= HAYSTACK GYPSUM], basal member of Blaine Formation
40	810	3316	Mudstone, reddish brown, sharp upper contact
41	222	3538	Gypsum [= CEDARTOP GYPSUM], sharp upper contact
42	310	3848	Mudstone, reddish brown, sharp upper contact
43	5	3853	Dolomite, gray

The dominant lithology of the upper Flowerpot Formation in my measured section is a reddish-brown mudstone to siltstone making up ~65% of the outcrop of study. About 25% of the measured outcrop is a dark gray (unweathered) mudstone. It is common for both red and gray mudstones to be intercalated with thin crinkly beds of gypsum. In addition, gypsum stringers are common throughout the outcrop. Thicker beds of gypsum, some extensive enough to bear names (e.g., Kiser and Chaney gypsums), comprise ~3% of the measured section. Thin beds of dolomite are also recognized in the Flowerpot Formation and comprise less than 1%. In the subsurface, bedded halite is reported to be present (Johnson, 1982), but no trace is apparent in my section.

When initially scouting this locality, preliminary samples (OPC 2218-2225) were taken from a conspicuous greenish mudstone with green minerals weathering out (= 'copper interval', Bed 20, Figure 10) and proved to be palynological productive. Slides (with catalog numbers 31510-31536) from these samples were used to survey palynological diversity but were not part

of the quantitative analyses; images of several pollen and spore types come from these survey samples. According to Johnson (Johnson and Croy, 1976), the Meadows copper bed is "closely related, or in part equivalent, to a 6-inch-thick spore-bearing shale immediately below the Kiser Gypsum Bed (Johnson and Croy, 1976, p. 8)" referring specifically to Wilson's site about 8.5 km west-northwest of my locality. There is no Kiser gypsum member or visible copper mineralization at Wilson's site. However, a correlative stratigraphic position is inferred between Wilson's productive horizon and my 'copper interval' on the basis of the position of both approximately 30 ft below the base of the Haystack Gypsum of the overlying Blaine Formation. My 'copper interval' is tentatively considered to be stratigraphically equivalent to the Meadows copper bed located at the Creta copper mine. Bed 20—the 'copper interval'—was more intensively sampled to study the pollen and spores, and their variations in diversity and abundance, in this interval. Samples below, in, and above Bed 20 were taken at about 2-4 cm intervals (see description of section above). From this later intensive sampling, 10 of the 30 samples were selected for initial palynological investigation to provide a snapshot of variation and trends among them (Figure 13). My intent was to analyze the remaining samples but limitations and restrictions due to the COVID-19 pandemic prevented additional analyses. Overall, my palynological investigation is based on samples in my section from a 1.34 m interval around Bed 20.

Samples for palynology were submitted to Global Geolab, Ltd. for palynological preparation. Standard processing techniques include grinding the rock samples to powder consistency and bathing them in a series of acidic washes of HF and HCl to remove the siliceous rock matrix and all extraneous organic matter. The remaining residue of resistant sporopollenin of the exine of palynomorphs is mounted on microscopic slides. For a more detailed account of

the process of maceration and slide preparation, see Traverse (2007) and Jones and Rowe (1999).

The prepared slides were viewed on an Olympus BX50 with a Canon EOS Rebel T1i camera. Photos were taken of all samples through a 40X lens and captured at 4700x3100 resolution using EOS Utility software. Early palynologists suggested that 200 grains were sufficient for pollen analysis (Barkley, 1934). However, in view of the dominance of *Lueckisporites* sp. on most slides, I counted an extra 100 grains to try to include additional taxa in each sample. Slide counts were performed by identifying 300 palynomorphs (or all on an entire slide if preservation was very poor) at the lowest taxonomic classification as possible based upon comparisons of previous research on Permian palynology, including but not limited to Wilson (1962), Clapham (1970), and Morgan (1967). Measurements of the palynomorphs were taken from micrographs and included the following measurements modified after Traverse (1988):

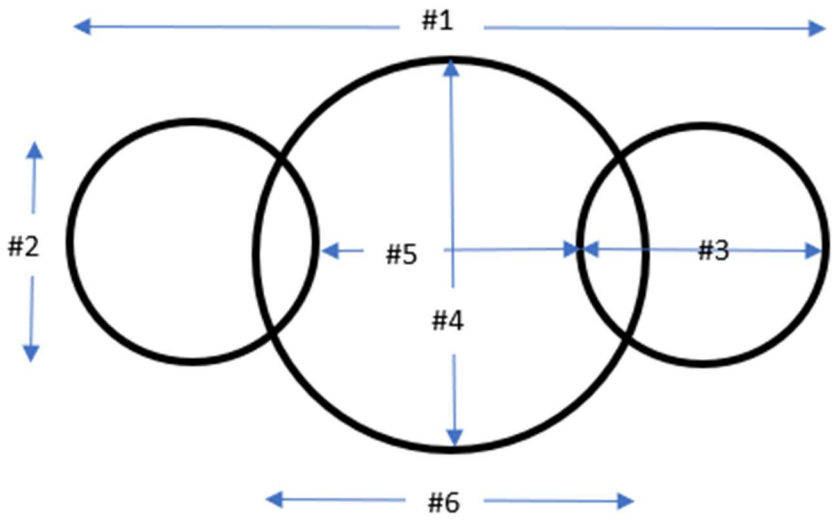

#1 Overall length

#2 Saccus width

#3 Saccus height

#4 Corpus width

#5 Distance between sacci

#6 Corpus length

RESULTS

TAXONOMIC DIVERSITY

In total from all samples collected at this site, including samples from the preliminary survey (OPC 2218-2225) but not included in quantitative counts, there were 47 "species"—25 pollen types representing seed plants, 18 spore types representing free-sporing plants (e.g., ferns, mosses, lycopsids), three fungal types and one inferred algal type (see Table 1 and Plates).

Spores—including monolete (one species overall) and trilete species (17 species overall)—ranged in diversity from two to nine species per counted sample (including those found outside of 300-grain count by scanning the whole slide). The diversity of all seed plants in samples ranged from 2 to 13 species per sample (including 'outside of count'). Seed plant pollen was divided into two groups: striate and non-striate. Striate seed plant pollen included bisaccate pollen, such as *Lueckisporites sp., Strotersporites* sp.*,* and *Hamiapollenites* sp.*,* and other striate forms, e.g., *Vittatina spp.* The diversity of striate grains ranged in number from one to eight species per sample, with nine taxa overall. The diversity of non-striate seed plant pollen, including bisaccate and monosaccate pollen, ranged from one to six species per sample, with 16 species overall. Diversity of non-plant palynomorphs—fungal or algal spores—ranged from one to four species. *Psophosphaera*? sp. has a disputed affinity but is here categorized as an algal spore.

The highest spore diversity was observed in sample OPC 2241 with nine species identified. Striate pollen diversity were highest in four samples with seven species located in

samples OPC 2227, OPC 2235, OPC 2241, and OPC 2248. Non-striate pollen diversity was highest at six species identified in each of samples OPC 2235, OPC 2248, and OPC 2250. All samples contained *Psophosphaera*. The upper three samples, OPC 2253, 2254, and 2255, contained the lowest diversity of spores with one or two species each. Similarly, the diversity count was lowest for non-striate seed pollen in samples OPC 2253 and 2254—each having one species—and sample OPC 2255 having only two. Sample OPC 2254 contained the lowest diversity for striate bisaccate pollen with the single genus *Lueckisporites* identified. Samples OPC 2253 and 2254 were the only samples to contain fungal spores.

ECOLOGICAL ABUNDANCE

A 300-specimen count was attempted for all ten slides (Table 2). Beginning with the lowest sample from Bed 20 'copper interval', OPC 2227, the abundance of specimens was sparse with only 82 specimens at the genus-level identified. *Lueckisporites* sp. composed 61.0% of the population. Combined with other striate bisaccates and non-striate bisaccates, whose percentages were 12.2% and 11.0%, respectively, the entire sample is composed 84.2% bisaccate pollen. *Vittatina* spp. composed 3.7% and was the only other known pollen identified. Monolete and trilete spores composed 3.7% of the population. *Psophosphaera* sp., whose affinities are uncertain, made up 8.5% of the sample. No fungal spores or monosaccate pollen were identified.

In sample OPC 2235, a 300-specimen count was achieved. *Lueckisporites* sp. composed 79.3% of the population and combined with other striate bisaccates at 7.3% and non-striate bisaccates at 4.7%, the entire count is 91.3% bisaccates. Monosaccates and *Vittatina* spp. make up 1% and 4%, respectively, while trilete and monolete spores constitute just over 2%. *Psophosphaera* sp. is 1% of the population and there were no fungal spores identified.

Lueckisporites sp. comprised 81.3% of sample OPC 2241 where a 300 count of specimens were identified. Other striate bisaccates and non-striate bisaccates make up 6.3% and 3.7%, respectively, combining with *Lueckisporites* sp. to comprise 91.3% as bisaccates. Other pollen included a single specimen of monosaccate and 12 specimens of *Vittatina* spp. composing 0.3% and 4.0%, respectively. Monolete and trilete spores combined to make up 2.7% of the population. No fungal spores were identified.

In sample OPC 2247, a 300-count was attained and *Lueckisporites* sp. composed 80% of the population while striate bisaccates and non-striate bisaccates made up 8.7% and 5.7%, respectively. All bisaccates made up 94% of the sample counted. *Vittatina* spp. was 2.7% of the population and no monosaccates were identified. Spores composed 1.7% and *Psophosphaera* sp. was 1.0%. No fungal spores were identified.

Lueckisporites sp. made up 79.3% of the 300 counted grains in sample OPC 2248. Other striate bisaccates made up 9% and non-striate bisaccates comprised 6.3%, combining with *Lueckisporites* sp. to compose 94.6% of the count as bisaccate pollen. Monosaccate pollen composed 0.7% and *Vittatina* spp. were 2.0% of the total. Spores and *Psophosphaera* sp. composed 1.7% and 1.0%, respectively. No fungal spores were present in the count.

In sample OPC 2250, a 300-specimen count was attained and *Lueckisporites* sp. made up 71.7% of the population. Other striate bisaccates comprised 12.3% and 9.3% were non-striate bisaccates and together with *Lueckisporites* sp. comprised 93.3% of the entire count. Monosaccate pollen and *Vittatina* spp. composed 0.3% and 3.7%, respectively. Spores and *Psophosphaera* sp. each made up 1.3%. No fungal spores were identified.

Lueckisporites sp. constituted 75.3% of sample OPC 2251 where a 300-specimen count was attained. Together with other striate bisaccates at 10.7% and non-striate bisaccates at 7.7%,

bisaccate pollen accounted for 93.7% of the population. Monosaccate pollen accounted for 0.7% and *Vittatina* spp. was 2.0% of the count. Spores and *Psophosphaera* sp. made up 2.7% and 1.0%, respectively. No fungal spores were present in the count.

In sample OPC 2253, a 300-speciment count was not attained and only 107 specimens were identified. *Lueckisporites* sp. composed 20.6%, other striate bisaccates made up 1.9%, and non-striate bisaccates were 0.9% of the population. The bisaccates combined to be 23.4% of the population. *Vittatina* spp. comprised 3.7% and no monosaccates were found. Spores and *Psophosphaera* sp. made up 2.7% and 0.9%, respectively. Fungal spores identified as *Brachysporisporites* comprised the majority of specimens identified with a total of 69.2%.

Sample OPC 2254, the uppermost sample below the Kiser gypsum member, contained 145 identified specimens. *Lueckisporites* sp. composed 9.0% and no other striate bisaccates were found. Non-striate bisaccates found made up 1.4% and combined with *Lueckisporites* sp., bisaccates accounted for 10.4% of the specimens found. No monosaccate pollen or *Vittatina* spp. were identified. Spores composed 4.8% and *Psophosphaera* sp. was 1.4% of the specimens. Fungal spores identified as *Paleomycites* sp. accounted for 83.4% of the population identified.

The uppermost sample of Bed 20 (OPC 2255) and above the Kiser gypsum, contained only 67 identified specimens. *Lueckisporites* sp. accounted for 74.6% and other striate bisaccates and non-striate bisaccates composed 1.5% and 13.4%, respectively. Combined, these bisaccate pollen comprised 89.5% of the count. Monosaccate pollen made up 1.5% and *Vittatina* spp. was 4.5% of the identified specimens. Spores and *Psophosphaera* sp. made up 3.0% and 1.5%, respectively. No fungal spores were present in the count.

XRF COPPER ANALYSIS

Results of a preliminary XRF analysis of three samples from Bed 20—OPC 2228, OPC 2245, and OPC 2251 (two replicates of each sample)—representing the lower, middle and upper parts of the "copper interval" were tested for copper content. The lowest sample, OPC 2228, yielded an average copper content of 0.078% (0.0568%, 0.0991%); the middle sample, OPC 2245, yielded an average copper content of 1.3% (0.5685%, 1.9864%); and the upper sample, OPC 2251, yielded an average copper content of 0.14% (0.0398%, 0.2432%)). OPC 2228 was processed for pollen, but was largely unproductive, yielding only six complete, identifiable grains—5 *Lueckisporites* sp. and 1 trilete spore. The nearest sample to OPC 2228 was OPC 2227 (from 2 cm below but in Bed 19) and contained only 82 identifiable palynomorphs. OPC 2245 was palynologically very productive, but a quantitative count was not conducted as part of the original ten samples; visually, it was overwhelmingly dominated by *Lueckisporites* sp. The nearest counted sample to OPC 2245 was OPC 2247 (from 5 cm above) and was composed of ~80% *Lueckisporites* sp. with numerous other taxa of both pollen and spores. OPC 2251 contained over 300 identifiable palynomorphs and was also composed of ~80% *Lueckisporites* sp. with numerous other taxa of both pollen and spores. There is no clear relationship —linear or threshold—between copper content and palynological recovery based on only three samples. OPC 2245 has approximately 8.5x more copper than OPC 2251 but demonstrates no marked difference in palynological recovery or estimated diversity/abundance. Further XRF analyses and exploration of the relationship between copper content and palynology were curtailed by COVID-19 pandemic.

DISCUSSION

Climate and vegetation are closely linked, and palynology can supplement other geological data to provide a glimpse into the palaeoecological conditions during the deposition of the Flowerpot Formation. However, based solely on dispersed pollen and spores in this area, it is not possible to determine the exact vegetational cover of an area making palaeoecological reconstruction difficult. Certain assumptions can be made, however, keeping in mind various caveats. First, no floral macrofossils have been recovered from the Flowerpot Formation, and, by extension, no parent plant can be assigned directly to the pollen and spores found. Although some pollen/spore taxa found in this study have been recognized, in situ, in reproductive structures of identified plants in other regions of Pangea, strong similarity of form, at least when using light microscopy, is common among plant miospores (Traverse, 2007). In addition, multiple morphotaxa occasionally have been found in the same pollen sacs. Lindstrom et al. (1997) identified 2656 pollen grains from sporangia of *Glossopteris,* of which ~96% were haploxylonoid (assignable to the genus *Protohaploxipinus*), ~4% were diploxylonoid (assignable to the genus *Striatopodocarpidites*), and even a small amount, 0.2%, were monosaccate (assignable to the genus *Striomonosaccites*). *Protohaploxipinus* was found in fair abundance in the current study site that is located in western equatorial Pangea where *Glossopteris* is unknown. To complicate matters further, different plants distribute varying amounts of pollen, and they are not always uniformly distributed or preserved (Looy and Hotton, 2014). Other factors that can influence the amount of dispersed pollen and spores include height and location of parent plant relative to the depositional area, method of delivery, and prevailing air currents and rain patterns (Looy and Hotton, 2014). With these caveats in mind, palynological data provide broad taxonomic and paleoecological patterns, and dispersed pollen and spores show

characteristics of higher taxonomic groups (e.g., families and genera) rather than individual species. Likewise, these variations in diversity and abundance may reflect broad ecologically important fluctuations in vegetational composition related to climatic changes.

In contrast to macrofossils that can preserve local floras on the scale of square meters, the nature of delivery of dispersed pollen and spores to a depositional site can mix many taxa across varying local habitats on the scale of many square kilometers (Burnham et al., 1992). And while the spatial resolution is obscured, the ability to sample from an outcrop on a cubic centimeter scale that encompasses such a wide area effectively captures regional vegetational patterns (Burnham et al., 1992).

Bisaccate pollen are well-established by the late Carboniferous and early Permian, but they (especially taeniate forms) came to dominate palyno-assemblages nearly worldwide by the middle-to-late Permian and into the Triassic. The characteristic taeniae (= horizontal and/or vertical bands of cell walls that appear thicker) are believed to have a harmomegathic function adapted to swell and contract in relation to available moisture and are associated with seasonally dry to arid habitats (Zavialova et al., 1996). The ubiquity and high abundance of taeniate bisaccate pollen from the current study site support an interpretation of a seasonally dry or arid environment with dry-tolerant plants of a coniferalean affinity nearby (as per Wilson, 1962). However, the persistence of pteridophytic spores is evidence of wetter substrates somewhere on a heterogenous landscape, but their high diversity and contrasting low abundance suggests that much of this spore input was from some significant distance.

Wilson's (1962) sample OPC 1 most closely resembles the current study in both diversity (numerous shared taxa) and abundance, with bisaccates including *Lueckisporites,* making up over 85% of the specimen count in both studies. My samples were taken at approximately the

same stratigraphic position (relative to the overlying Haystack Gypsum of the Blaine Formation) as Wilson's, with about 8.5 km separating them.

The marked increase in diversity and abundance of palynomorphs for Clapham (1970) and Morgan (1967) compared to the current study can be attributed both to the wider geographic and stratigraphic range of samples and to reporting. Clapham (1970) did not report individual sample diversity and reported qualitative (e.g., rare, common) abundance for only *some* major taxa in individual samples. All of Clapham's samples were taken in the upper ten to 35 feet of the Flowerpot Formation in Oklahoma clustered in two areas 280 km apart—around Woods, Major, and Woodward Counties in NW Oklahoma and around Greer and Beckham Counties in SW Oklahoma. Based on his findings, Clapham (1970) divided his samples into two distinct assemblages and he reported quantitative abundances of major morphological groups for the average of all samples assigned to each assemblage (text-figure 3 of Clapham, 1970). One he denoted as Assemblage G, with *Lueckisporites* and other bisaccate pollen accounting for more than 85% of the population. Clapham's Assemblage G most closely resembles the current study site in the overwhelming abundance of *Lueckisporites* and other bisaccates. Clapham's (1970) second assemblage, Assemblage F, shows an increase in abundance and diversity of spores as well as an increase of what he interpreted as hydrophilous pollen: *Psophosphaera* and *Paludospora. Lueckisporites* and other bisaccates still figure prominently in Clapham's Assemblage F but at a much lower percentage (less than 50%). Clapham interpreted this reduction in bisaccates and concomitant increase in spores as a regressive interval where more low-lying land space (marshes and swamps) was available for habitation by a spore-producing flora. No indication of Clapham's Assemblage F was identified at the current study site because

all samples showed an abundance of *Lueckisporites* (notwithstanding low-recovery samples dominated by fungi).

Morgan's (1967) samples came from a wider temporal range that extended from the Flowerpot into Blaine and Dog Creek Formations. Like Clapham, Morgan did not report individual sample diversity and only abundance of some major taxa. Morgan's samples in the Flowerpot Formation closely resemble the current study site, Wilson's sample, and Clapham's Assemblage G by possessing an overwhelming abundance of bisaccate pollen. There were, however, four distinct horizons in the middle Blaine that showed an increase in *Psophosphaera* with a corresponding decrease in bisaccate abundance, like that of Clapham's Assemblage F.

One of the more interesting discoveries at my study site is the sudden appearance of inferred fungal spores in the two samples underlying the Kiser Gypsum. The fungal spores and disarticulated hyphae identified in OPC 2253 and 2254 belong to the genera *Paleomycites*? and *Brachysporisporites*?, respectively. It should be noted that research and data on fungal spores in the Paleozoic is scant at best and the identified fungal spores have not previously been recognized in the Flowerpot Formation. Although *Reduviasporonites* from the Flowerpot was initially thought to be of fungal origin (Wilson 1962, Elsik 1999), it is now considered to represent an alga (Foster et al. 2002). These two samples also showed a significant reduction in pollen and spore abundance to 32 total specimens in OPC 2253 and 24 total specimens in OPC 2254 in addition to the low total count. A spike in fungal spores has been identified at various locations around the world at P-Tr boundary and interpreted (Eshet et al 1995; Visscher et al 1996) to be evidence of global ecological stress associated with the Permian extinction. However, this is not without controversy as some researchers have asserted these palynomorphs are algal and not fungal (Foster et al., 2002). Nevertheless, if the appearance of fungal spores

with a concomitant decrease in plant pollen and spores is not a taphonomic issue, then by analogy with the Permian-Triassic Boundary, it could indicate some type of environmental stress associated with increased evaporation rates preceding the formation of a gypsum.

Pollen and spores are dispersed by wind, water, and/or insects. Their sporopollenin exines are extremely amenable to preservation if they are not exposed to an oxidative environment for too long and are protected from microbial action at the site of deposition. Oxidation occurs either by the pollen or spore being deposited on surfaces exposed directly to oxygen or by oxygenated groundwater leaching into the palynomorph bearing strata. Extremely dry or wet conditions, colder temperatures, and acidic environments help inhibit microbial growth. Another lesser-known factor in the preservation of pollen and spores could by the presence of copper salts in the soil that act as a fungicide. The association between pollen and spores has been noted Hagni and Gann (1976) as copper sulfides (chalcocite) replacing spore bodies. Although this does not account for why all the spores and pollen were replaced by copper, the fact that copper does exist in the reduced strata where palynomorphs are found could be a factor in their preservation (King, 1975).

CONCLUSIONS

The Flowerpot Formation was deposited as a progradational unit building westward into a shallow, restricted inland sea characterized by hypersaline conditions with limited fauna. The shallow sea was restricted to the west by a narrow inlet to the open ocean in the Midland and Delaware Basin area. The shoreward side consisted of wide, flat alluvial coastal plain comprising refugia of salt marshes, lagoons, and mudflats that contained pteridophytic flora near the shoreline although distant from the depositional area of my site. A conifer-rich flora dominated

and as aridity increased in the area, sabkha environments developed. The oscillation of sea level, combined with increasing aridity, allowed for the deposition of evaporites in increasing frequency and abundance seen in my section and more broadly in upper Flowerpot and Blaine Formations in Oklahoma and Kansas. A low gradient rise continued to the east to uplands in the Ozarks, Ouachitas and even Appalachian Mountains that were the source for the clastic sediments introduced to the Flowerpot Formation transported by low competence streams and possibly monsoonal winds (Sweet et al., 2013). Small fluctuations in sea level would have had a significant impact over the broad, low relief area extending into areas of the Hugoton Embayment (e.g., saline pans, lakes) and northern Anadarko Basin (Benison and Goldstein, 2001). As further retreat of the sea continued to the west, more drought tolerant flora with bisaccate pollen came to dominate the area.

With increasing aridity and the concomitant encroachment of the sabkha provided the correct combination of materials and conditions needed for copper mineralization in the Flowerpot Formation. Following Smith's (1976) model of evaporative sabkha discharge, the deposition of carbonaceous material (e.g., pollen, spores, woody fragments) was subsequently followed by formation of evaporites (in this case, gypsum). Bacterial reduction of the organic material produced a layer of sulfide that copper-rich waters (from leached red beds) passed through by means of evaporative pumping, thereby precipitating copper minerals. The deposition of organic matter in the form of pollen and spores may have been necessary for the precipitation of copper, which in turn may have favored long-term preservation of the original pollen and spores.

SYSTEMATIC PALYNOLOGY

Trilete spore type 1

Plate 1, Figure 1

Description: Spore; trilete; amb sub-round to sub-triangular; exine micropitted; laesurae extend full length of equatorial diameter.

Dimensions: Diameter 40 microns at widest point.

Trilete spore type 2

Plate 1, Figure 2

Description: Spore; trilete; amb round; exine psilate to weakly granulate; laesura extending about ¼ of equatorial diameter.

Dimensions: Diameter 12.5 microns.

Trilete spore type 3

Plate 1, Figure 3

Description: Spore; trilete; amb round; exine psilate; laesurae extend full length of of equatorial diameter.

Dimensions: Diameter 22.5 microns.

Calamospora sp.

Plate 1, Figure 4

Description: Spore; trilete; amb sub-round; exine predominantly psilate with some micropitting; laesurae extend ~1/3 of of equatorial diameter.

Remarks: Although simple and largely without ornament, this form conforms to the circumscription of the genus *Calamospora*.

Dimensions: Diameter 75 microns

Trilete spore type 5

Plate 1, Figure 5

Description: Spore; trilete; amb round; exine verrucate; thick outer wall; laesurae extend ~2/3 of equatorial diameter.

Dimensions: Diameter 75 microns; outer wall ~2.5 microns.

Trilete spore type 6

Plate 1, Figure 6

Descriptions: Spore; trilete; amb round; exine granulate to weakly verrucate; laesurae ~2/3 of of equatorial diameter.

Dimensions: Diameter 55 microns.

Trilete spore type 7

Plate 2, Figure 1

Description: Spore; trilete; amb round; exine predominantly psilate with some foveolate structures; thick spore wall; laesurae extend ¾ distance of of equatorial diameter.

Dimensions: Diameter 62.5 microns; spore wall ~2.5 microns thick.

Trilete spore type 8

Plate 2, Figure 2

Description: Spore; trilete; amb sub-triangular; exine verrucate to gemmate; laesurae extend full length of of equatorial diameter.

Dimensions: Diameter 32.5 microns.

Trilete spore type 9

Plate 2, Figure 3

Description: Spore; trilete; amb sub-round; exine granulate; straight laesurae extend ¾ distance of surface area.

Dimensions: Diameter 30 microns.

Trilete spore type 10

Plate 2, Figure 4

Description: Spore; trilete; amb sub-triangular; exine granulate to weakly verrucate; laesurae extend full distance of equatorial diameter.

Dimensions: Diameter 37 microns.

Trilete spore type 11

Plate 2, Figure 5

Description: Spore; trilete; amb round; exine psilate; thick spore wall; straight laesurae extend ~1/2 distance to equatorial diameter.

Dimensions: Diameter 27.5 microns; outer wall ~2 microns.

Trilete spore type 12

Plate 2, Figure 6

Descriptions: Spore; trilete; amb sub-triangular; exine clavate; laesurae extend >1/2 distance to equatorial diameter.

Dimensions: Diameter 42.5 microns at widest point including ornament; amb is 32.5 microns; ornamentation ~5 microns tall.

Trilete spore type 13

Plate 3, Figure 1

Descriptions: Spore; trilete; amb sub-triangular with concave sides; exine psilate with some micro-pitting.

Dimensions: Diameter 30 microns at widest points.

Trilete spore type 14

Plate 3, Figure 2

Description: Spore?; no visible laesura; amb round; exine rugulate

Remarks: Although apparently lacking a laesura, this form resembles other round and rugulate spores that are trilete.

Dimensions: Diameter 27 microns.

Trilete spore type 15

Plate 3, Figure 3

Description: Spore?; no visible laesura; amb round; exine verrucate.

Remarks: Although apparently lacking a laesura, this form resembles other round and verrucate spores that are trilete.

Dimensions: Diameter 27.5 microns.

Trilete spore type 16

Plate 3, Figure 4

Description: Spore?; no visible laesura; amb round; exine echinate; thick outer wall.

Dimensions: Diameter 35 microns; outer wall ~2 microns thick.

Trilete spore type 17

Plate 3, Figure 5

Description: Spore?; no visible laesura; amb round; exine reticulate.

Remarks: Has appearance of a thick reticulate sheath (~2 microns) surrounding an inner body.

Dimensions: Diameter 40 microns.

Laevigatosporites sp.

Plate 3, Figure 6

Description: Spore; monolete laesura; amb round; exine psilate to micropitted; thick outer wall.

Remarks: Numerous species of *Laevigatosporites* are recognized, but many are differentiated on the basis of size alone.

Dimensions: Diameter 35 microns; outer wall ~1 micron thick.

Protohaploxypinus? sp. 1

Plate 4, Figure 1

Description: Pollen; bisaccate; striate; round corpus; diploxylonoid; 7-9 horizontal taeniae; sacci reniform.

Remarks: *Protohaploxypinus*? sp. 1 is distinguished from *P*? sp. 2 by number of horizontal taeniae and the rounder shape of corpus and reniform shape of sacci. *Protohaploxypinus*? sp. 1 is distinguished from *P*? sp. 3 by both sides of sacci terminating on corpus.

Dimensions:

1. Overall length 32.5-40 microns
2. Saccus width 22.5-25.0 microns
3. Saccus height (not a specimen conducive to this measurement)
4. Corpus width 22.5-27.5 microns
5. Distance between sacci not a specimen conducive to this measurement
6. Corpus length 12.5-15.0 microns

Protohaploxypinus? sp. 2

Plate 4, Figure 2

Description: Pollen; bisaccate; striate; oval corpus; diploxylonoid; ~15 horizontal taeniae; taeniae fold (chevron) toward center of corpus; sacci crescent shaped.

Remarks: *Protohaploxypinus*? sp. 2 is distinguished from *P*? sp. 1 and *P*? sp. 3 by more horizontal taeniae and having an oval corpus and crescent shaped sacci.

Dimensions:

1. Overall length 40 microns

2. Saccus width 35 microns
3. Saccus height 12.5 microns
4. Corpus width 37.5 microns
5. Distance between sacci 13 microns
6. Corpus length 15 microns

Protohaploxypinus? sp. 3

Plate 4, Figure 3

Description: Pollen; bisaccate; striate; round corpus; ~8 horizontal taeniae; one end of saccus terminates on corpus, other end of saccus wraps around and appears to connect; sacci kidney shaped (reniform).

Remarks: *Protohaploxypinus? s*p.3 is similar to *P*? sp. 1 except the sacci are confluent on one side of corpus.

Dimensions:

1. Overall length 41 microns
2. Saccus width 22.5 microns
3. Saccus height 12.5 microns
4. Corpus width 37.5 microns
5. Distance between sacci 22.5 microns
6. Corpus length 25 microns

Alisporites sp. 1

Plate 4, Figure 4

Description: Pollen; bisaccate; non-striate; haploxylonoid; oval corpus; corpus micropitted to granulate.

Remarks: *Alisporites* sp 1 is distinguished from *A*. sp. 2 by having wider sacci and more clearly defined oval shape to corpus. *Alisporites* sp. 1 is distinguished from *A*. sp. 3 by also having wider sacci and less defined outline to corpus.

Dimensions:

1. Overall length 55-62.5 microns
2. Saccus width 32.5-35 microns
3. Saccus height 22.5-25 microns
4. Corpus width 32.5-35 microns
5. Distance between sacci 12.5 microns
6. Corpus length 22.5 microns

Alisporites sp. 2

Plate 4, Figure 5

Description: Pollen; bisaccate; non-striate; haploxylonoid; corpus micropitted.

Remarks: *Alisporites* sp. 2 is distinguished from *A*. sp. 1 and *A*. sp. 3 by having thinner sacci and a less developed corpus structure.

Dimensions:

1. Overall length 47.5 microns
2. Saccus width 36 microns
3. Saccus height 20 microns
4. Corpus width 36 microns

5. Distance between sacci 6 microns
6. Corpus length preservation too poor for measurement.

Alisporites sp. 3

Plate 4, Figure 6

Description: Pollen; bisaccate; non-striate; corpus and sacci micropitted to granulate.

Remarks: *Alisporites* sp. 3 is distinguished from *A*. sp. 1 and *A*. sp. 2 by having a more pronounced outline of corpus with a thicker corpus wall. *Alisporites* sp. 3 is also distinguished from *A*. sp. 1 and *A*. sp. 2 by having thinner sacci that do not seem to terminate as noticeably on corpus.

Dimensions:

1. Overall length 45-47.5 microns
2. Saccus width 30-35 microns
3. Saccus height 15-20 microns
4. Corpus width 27.5-35 microns
5. Distance between sacci 7.5-10 microns
6. Corpus length 20-25 microns

Limitisporites sp. 1

Plate 5, Figure 1

Description: Pollen; bisaccate; non-striate; corpus oval and psilate; sacci granulate; dilete laesura ~1/3 distance of corpus.

Remarks: *Limitisporites* sp. 1 is distinguished from *L*. sp. 2 by being smaller overall and having a dilete laesura.

Dimensions:

1. Overall length 62.5 microns
2. Saccus width 37.5 microns
3. Saccus height 17.5 microns
4. Corpus width 37.5 microns
5. Distance between sacci 20 microns
6. Corpus length 30 microns

Limitisporites sp. 2

Plate 5, Figure 2

Description: Pollen; bisaccate; non-striate; oval compressed corpus; corpus granulate to scabrate; sacci do terminate on corpus.

Remarks: *Limitisporites* sp. 2 is distinguished from *L*. sp. 1 by being larger overall and not possessing a laesura.

Dimensions:

1. Overall length 90-105 microns
2. Saccus width 55-65 microns
3. Saccus height 37.5-42.5 microns
4. Corpus width 51-60 microns
5. Distance between sacci 12.5-15 microns

6. Corpus length 32.5-40 microns

Bisaccate pollen type 1

Plate 5, Figure 3

Description: Pollen; bisaccate; non-striate; diploxylonoid; oval to sub-round corpus; corpus small in height and width compared to sacci; corpus micropitted to granulate.

Remarks: These specimens were grouped based upon being non-striate bisaccates with sacci extending much wider than corpus.

Dimensions:

1. Overall length 72.5-77.5 microns
2. Saccus width 47.5-50 microns
3. Saccus height 27.5-32.5 microns
4. Corpus width 35-40 microns
5. Distance between sacci 12.5-15 microns
6. Corpus length 22.5-32.5 microns

Bisaccate pollen type 2

Plate 5, Figure 4

Description: Pollen; bisaccate; non-striate; round corpus; corpus small compared to sacci; sacci appear to connect on both sides of corpus.

Remarks: This specimen was selected based upon being non-striate bisaccate with small corpus compared to sacci. Sacci appear confluent on both sides of corpus although this could be an artifact of preservation.

Dimensions:

1. Overall length 87.5 microns
2. Saccus width 55 microns
3. Saccus height 30 microns
4. Corpus width 35 microns
5. Distance between sacci 20 microns
6. Corpus length 30 microns

Bisaccate pollen type 3

Plate 5, Figure 5

Description: Pollen; bisaccate; non-striate; diploxylonoid; round corpus; corpus psilate to micropitted; thick outline of corpus; sacci reniform shape.

Remarks: This specimen was selected based on thick corpus wall and the size of the corpus in relation to the sacci.

Dimensions:

1. 72.5 microns
2. 62.5 microns
3. 35 microns
4. 47.5 microns
5. N/A
6. 42.5 microns

Bisaccate pollen type 4

Plate 5, Figure 6

Description: Pollen; bisaccate; non-striate; diploxylonoid; round corpus; corpus psilate; sacci granulate; dilete laesurae extending ~1/2 diameter of corpus.

Remarks: This specimen was selected based upon large corpus in relation to sacci and distinct dilete mark.

Dimensions:

1. Overall length 70 microns
2. Saccus width 42.5 microns
3. Saccus height N/A
4. Corpus width 45 microns
5. Distance between sacci N/A
6. Corpus length 42.5 microns

Bisaccate pollen type 5

Plate 6, Figure 1

Description: Pollen; bisaccate; non-striate; diploxylonoid; round corpus; corpus psilate to micropitted.

Remarks: Bisaccate pollen type 5 is distinguished from Bisaccate pollen type 3 by its larger, oval corpus, and from Bisaccate pollen type 6 by not having a laesura.

Dimensions:

1. 85-90 microns
2. 52.5-57.5 microns
3. 30-37.5 microns

4. 45-50 microns
5. 13 microns
6. 45-50 microns

Bisaccate pollen type 6

Plate 6, Figure 2

Description: Pollen; bisaccate; non-striate; diploxylonoid; round corpus; corpus psilate to micropitted; laesurae dilete extend approximately 1/2 corpus diameter.

Remarks: Bisaccate pollen type 6 is distinguished from Bisaccate pollen type 4 by its larger sacci with strongly curved proximal attachment and relatively smaller laesurae, and from Bisaccate pollen type 5 by having dilete laesurae.

Dimensions:

1. 85-90 microns
2. 52.5-57.5 microns
3. 30-37.5 microns
4. 45-50 microns
5. 13 microns
6. 45-50 microns

Bisaccate pollen type 7

Plate 6, Figure 3

Description: Pollen; bisaccate; non-striate; diploxylonoid; round corpus; corpus psilate to micropitted; trilete mark about 1/2 size of corpus.

Remarks: Bisaccate pollen type 7 is distinguished from all other bisaccate pollen herein by its trilete laesura.

Dimensions:

1. Overall length 65-92.5 microns
2. Saccus width 47.5-57 microns
3. Saccus height 25-35 microns
4. Corpus width 42.5-52.5 microns
5. Distance between sacci 15-25 microns
6. Corpus length 40-50 microns

Strotersporites sp.

Plate 6, Figure 4

Description: Pollen; bisaccate; striate; diploxylonoid; round to sub-round corpus; 8-14 horizontal taeniae; exine of taeniae bears a verrucate texture.

Remarks: These specimens were grouped based on overall larger size and the higher number of taeniae. At least one, and often two or more, taeniae pinch out usually around mid-point.

Dimensions:

1. Overall length 75-125 microns
2. Saccus width 50-70 microns
3. Saccus height 25-52.5 microns
4. Corpus width 42.5-60 microns
5. Distance between sacci 15 to 25 microns
6. Corpus length 45-57.5 microns

Bisaccate pollen type 9

Plate 6, Figure 5

Description: Pollen; bisaccate; striate; round corpus; corpus micropitted; 5-8 thick horizontal taeniae.

Remarks: These specimens are grouped base upon fewer and thicker taeniae which can be 5 to 7 microns thick.

Dimensions:

1. Overall length 70-75 microns
2. Saccus width 42.5-52.5 microns
3. Saccus height 25-30 microns
4. Corpus width 25-42.5 microns
5. Distance between sacci 15-17 microns
6. Corpus length 25-37.5 microns

Bisaccate pollen type 10

Plate 6, Figure 6

Description: Pollen; bisaccate; non-striate; diploxylonoid; corpus predominantly psilate to mildly micropitted; monolete laesura extending ~1/3 of way across corpus.

Remarks: These specimens were grouped based upon the monolete laesura, large sacci extending well beyond the corpus, and the relatively small size of the corpus.

Dimensions:

1. Overall length 70-95 microns

2. Saccus width 45-57.5 microns
3. Saccus height 30-40 microns
4. Corpus width 27.5-40 microns
5. Distance between sacci 5-10 microns
6. Corpus length 30-35 microns

Bisaccate pollen type 11

Plate 7, Figure 1

Description: Pollen; bisaccate; non-striate; diploxylonoid; corpus predominantly psilate to mildly micropitted.

Remarks: Bisaccate pollen type 11 is distinguished from all other bisaccate pollen by its very small corpus compared to its sacci.

Dimensions:

7. Overall length 70-95 microns
8. Saccus width 45-57.5 microns
9. Saccus height 30-40 microns
10. Corpus width 27.5-40 microns
11. Distance between sacci 5-10 microns
12. Corpus length 30-35 microns

Lueckisporites virkkiae Potonie and Klaus, 1954

Plate 7, Figures 2-6

Description: Pollen; bisaccate; striate; diploxylonoid; round to oblate corpus; two thicker taeniae separated by a striation; sometimes remnants of dilete or trilete laesura can be seen on "middle" striation.

Remarks: By far the most abundant genus at this site. Previous work by Klaus (1963) and Hart (1960, 1964) divided *Lueckisporites* into three species. Clapham (1970) disputed this segregation, although subsequent workers frequently recognize many species, even in one assemblage (e.g., Vazquez and Cesari, 2017). Although I recognize variation in saccus size and appearance (e.g., some have undulate margins) in my samples, I have assigned all of them to *L. virkkiae* presently.

Dimensions:

1. Overall length 50-80 microns
2. Saccus width 32.5-75 microns
3. Saccus height 15-30 microns
4. Corpus width 30-55 microns
5. Distance between sacci 12-22 microns
6. Corpus length 30-65 microns

Hamiapollenites perisporites (Jizba) Tschudy and Kosanke, 1965

Plate 8, Figures 1 & 2

Description: Pollen; bisaccate; striate; diploxylonoid; corpus round; sacci noticeably smaller than corpus; 6-8 horizontal taeniae, of which 1 to 2 will occasionally pinch out about ½ way across corpus; 1 to 3 thicker vertical taeniae.

Remarks: *Hamiapollenites* is distinguished by the possession of unambiguous sacci and one or more vertical taeniae. Specific identities are associated with the number of vertical taeniae and relative height of sacci compared to the corpus. Although Wilson (1962) described *Hamiapollenites saccatus*—the holotype for the genus—from the Flowerpot Formation about 8.5km from this site, none of the specimens that I recovered conform to his specific diagnosis which specifies 6-10 vertical taeniae ("ribs" of Wilson). All of my specimens possess 1-3 vertical taeniae thus conforming to *H. perisporites* (Jizba) Tschudy and Kosanke, 1965. The relative heights of the sacci are not considered worthy of specific separation based on observed variation in my samples.

Dimensions:

1. Overall length 42.5-50 microns
2. Saccus width 17.5-22.5 microns
3. Saccus height 12.5-17.5 microns
4. Corpus width 25-30 microns
5. Distance between sacci 15-22.5 microns
6. Corpus length 20-27.5 microns

Vittatina costabilis Wilson, 1962

Plate 8, Figure 3

Description: Pollen; round to sub-round to ellipsoidal; psilate to micropitted; 9-13 horizontal taeniae; 1 vertical taeniae that is thicker than horizontal taeniae.

Remarks: Occasional termination of horizontal taeniae and can occur before, at, or after midpoint; occasionally remnants of laesurae can be observed in middle of specimen, up

to about 1/4 length of specimen. My specimens are somewhat larger than described in the original description for the species, but otherwise conform in all characteristics.

Dimensions: Horizontal length 40-72 microns; vertical height 37-52 microns

Vittatina lata Wilson, 1962

Plate 8, Figure 4

Description: Pollen; ellipsoidal; micropitted to granulate; 5-9 horizontal taeniae; 2-9 vertical taeniae.

Remarks: Most vertical and horizontal taeniae terminate at end but occasionally will pinch out before, near, or after midpoint. *Vittatina lata* is reliably distinguished from *V. costabilis* by possession of multiple vertical taeniae that are both thin in terms of width along axis and thin in terms of apparent wall thickness. My specimens also differ slightly in size compared to Wilson's (1962) original description for the species, but otherwise conform in all characteristics.

Dimensions: Horizontal length 45-72 microns; vertical height 30-50 microns.

Potonieisporites sp. 1

Plate 8, Figure 5

Description: Pollen; monosaccate; round to subround to oblate; corpus usually round to sub round to sub-angular due to folding of corpus.

Remarks: *Potonieisporites* sp. 1 is distinguished from *P*. sp. 2 in not having a trilete mark on corpus.

Dimensions: 122 micrometers in diameter; corpus is 70 micrometers in diameter

Potonieisporites sp. 2

Plate 8, Figure 6

Description: Pollen; monosaccate; round to subround to oblate; corpus round to subround to subangular due to folding of corpus. Trilete laesurae extend about ¼ of the size of corpus.

Remarks: *Potonieisporites* sp. 2 distinguished from *P*. sp. 1 by having a trilete mark extending about ¼ of the size of corpus.

Dimensions: 131 micrometers in diameter; corpus is 68 microns in diameter.

Psophosphaera? sp.

Plate 9, Figure 1

Description: Algal spore?; spherical; folds in very thin-walled exine.

Dimensions: 37 microns in diameter.

Brachysporisporites? sp.

Plate 9, Figures 2-3

Description: Fungal spore; generally ovate shape; mostly opaque; septa divide specimen into segments; distal end broad and rounded; proximal end tapered to flat termination; possible pore opening.

Remarks: There are numerous specimens of this type having varying number of constrictions/ septae. All are conspicuously opaque/black in my samples.

Dimensions: 42-55 microns in length; 27.5-30 microns in width.

Paleomycites? sp.

Plate 9, Figures 4-5

Description: Fungal spore; rounded to subrounded to oval in shape; show some signs of micropitting; hyphae protruding from spore body.

Remarks: All of these specimens have hyphae extending from spore body.

Dimensions: 38-85 microns in diameter; hyphae variable in length.

Fungal spore type 3

Plate 9, Figure 6

Description: Fungal spore(?); rounded to subrounded to oval in shape; predominantly psilate with occasional micropitting.

Remarks: These specimens occasionally have hyphae extending out from spore body but are distinguished from *Paleomycites* in having a thicker outer wall.

Dimensions: 50 microns in diameter.

REFERENCES

Benison, Kathleen Counter, and Robert H. Goldstein. "Evaporites and siliciclastics of the Permian Nippewalla Group of Kansas, USA: a case for non-marine deposition in saline lakes and saline pans." *Sedimentology* 48, no. 1 (2001): 165-188.

Berner, Robert A. "Chemical weathering and its effect on atmospheric CO_2 and climate." *Chemical weathering rates of silicate minerals* (2018): 565-584.

Blakey, Ronald C. "Gondwana paleogeography from assembly to breakup—A 500 my odyssey." *Geological Society of America Special Papers* 441 (2008): 1-28.

Burnham, Robyn J., Scott L. Wing, and Geoffrey G. Parker. "The reflection of deciduous forest communities in leaf litter: implications for autochthonous litter assemblages from the fossil record." *Paleobiology* 18, no. 1 (1992): 30-49.

Chaloner, William G., and Jennifer C. McElwain. "The fossil plant record and global climatic change." *Review of Palaeobotany and Palynology* 95, no. 1-4 (1997): 73-82.

Clapham, Jr., W. B. "Permian miospores from the Flowerpot Formation of western Oklahoma." *Micropaleontology* 16, no. 1 (1970): 15-36.

Clapham, Jr., W. B. "Nature and paleogeography of middle Permian floras of Oklahoma as inferred from their pollen record." *The Journal of Geology* 78, no. 2 (1970): 153-171.

Clement-Westerhof, Jopie A. "In situ pollen from gymnospermous cones from the Upper Permian of the Italian Alps—a preliminary account." *Review of Palaeobotany and Palynology* 17, no. 1-2 (1974): 63-73.

Cox, Dennis P., David A. Lindsey, Donald A. Singer, and Michael F. Diggles. *Sediment-hosted copper deposits of the world: Deposit models and database*. Reston, VA, USA: US Department of the Interior, US Geological Survey, 2007.

Cragin, F. W. "Permian system in Kansas: Colorado College Studies, vol. 6." (1896): 33-38.

Crowell, J. C. (1995). The ending of the late Paleozoic ice age during the Permian Period. In *The Permian of Northern Pangea* (pp. 62-74). Springer, Berlin, Heidelberg.

Davidson, C. F. "A possible mode of origin of strata-bound copper ores." *Economic Geology* 60, no. 5 (1965): 942-954.

DiMichele, William A., and Bret S. Beall. "Flora, fauna, and paleoecology of the Brazil Formation of Indiana." *Rocks & Minerals* 65, no. 3 (1990): 244-250.

DiMichele, William A., Hermann W. Pfefferkorn, and Robert A. Gastaldo. "Response of Late Carboniferous and Early Permian plant communities to climate change." *Annual Review of Earth and Planetary Sciences* 29, no. 1 (2001): 461-487.

DiMichele, William A., Dan S. Chaney, William H. Dixon, W. John Nelson, and Robert W. Hook. "An Early Permian coastal flora from the central basin platform of Gaines County, west Texas." *Palaios* 15, no. 6 (2000): 524-534.

DiMichele, William A., Sergius H. Mamay, Dan S. Chaney, Robert W. Hook, and W. John Nelson. "An Early Permian flora with Late Permian and Mesozoic affinities from north-central Texas." *Journal of Paleontology* 75, no. 2 (2001): 449-460.

DiMichele, William A., Neil J. Tabor, and Dan S. Chaney. "Outcrop-scale environmental heterogeneity and vegetational complexity in the Permo-Carboniferous Markley Formation of North Central Texas." *The Nonmarine Permian: New Mexico Museum of Natural History and Science Bulletin* 30 (2005): 60-66.

DiMichele, William A. "Wetland-dryland vegetational dynamics in the Pennsylvanian ice age tropics." *International Journal of Plant Sciences* 175, no. 2 (2014): 123-164.

DiMichele, William A., Arden R. Bashforth, Howard J. Falcon-Lang, and Spencer G. Lucas. "Uplands, lowlands, and climate: Taphonomic megabiases and the apparent rise of a xeromorphic, drought-tolerant flora during the Pennsylvanian-Permian transition." *Palaeogeography, Palaeoclimatology, Palaeoecology* 559 (2020): 109965.

Elsik, William C. "*Reduviasporonites* Wilson 1962: synonymy of the fungal organism involved in the Late Permian crisis." *Palynology* 23 (1999): 37-41.

Eshet, Yoram, Michael R. Rampino, and Henk Visscher. "Fungal event and palynological record of ecological crisis and recovery across the Permian-Triassic boundary." *Geology* 23, no. 11 (1995): 967-970.

Fay, Robert O. "The Blaine and Related Formations of Northwestern Oklahoma." *Oklahoma Geological Survey Bulletin* 98 (1964): 1-238.

Fay, Robert O. "Bibliography of copper occurrences in Pennsylvanian and Permian red beds and associated rocks." *Oklahoma Geological Survey Special Publication* (2000): 1.

Foster, Clinton B., M. H. Stephenson, Craig P. Marshall, Graham A. Logan, and P. F. Greenwood. "A revision of *Reduviasporonites* Wilson 1962: description, illustration, comparison and biological affinities." *Palynology* 26, no. 1 (2002): 35-58.

Gastaldo, Robert A., William A. DiMichele, and Hermann W. Pfefferkorn. "Out of the icehouse into the greenhouse: a late Paleozoic analogue for modern global vegetational change." *GSA Today* (1996).

Gilbert, M. Charles. "Speculations on the origin of the Anadarko Basin." In *Basement Tectonics 7*, pp. 195-208. Springer, Dordrecht, 1992.

Giles, Jessica M., Michael J. Soreghan, Kathleen C. Benison, Gerilyn S. Soreghan, and Stephen T. Hasiotis. "Lakes, loess, and paleosols in the Permian Wellington Formation of

Oklahoma, USA: implications for paleoclimate and paleogeography of the Midcontinent." *Journal of Sedimentary Research* 83, no. 10 (2013): 825-846.

Goddéris, Yves, Yannick Donnadieu, Sébastien Carretier, Markus Aretz, Guillaume Dera, Mélina Macouin, and Vincent Regard. "Onset and ending of the late Palaeozoic ice age triggered by tectonically paced rock weathering." *Nature Geoscience* 10, no. 5 (2017): 382-386.

Golonka, Jan, and David Ford. "Pangean (late Carboniferous–Middle Jurassic) paleoenvironment and lithofacies." *Palaeogeography, Palaeoclimatology, Palaeoecology* 161, no. 1-2 (2000): 1-34.

Greenwood, David R., and S. K. Donovan. "The taphonomy of plant macrofossils." *The processes of fossilization* (1991): 141-169.

Hagni, Richard D., and Delbert E. Gann. "Microscopy of copper ore at the Creta Mine southwestern Oklahoma." Pp. 40-50 in Johnson, Kenneth S., and Rosemary L. Croy, eds. *Stratiform Copper Deposits of the Midcontinent Region: A Symposium*. Oklahoma Geological Survey Circular 77. (1976).

Hansen, Robert F. "Areal geology of the southwest Mangum area, Oklahoma." PhD diss., University of Oklahoma, 1958.

Haynes, D. W. "Stratiform copper deposits hosted by low-energy sediments; I, Timing of sulfide precipitation, an hypothesis." *Economic Geology* 81, no. 2 (1986): 250-265.

Heckel, Philip H., Aleksandr S. Alekseev, James E. Barrick, Darwin R. Boardman, Natalya V. Goreva, Tamara I. Nemyrovska, Katsumi Ueno, Elisa Villa, and David M. Work. "Cyclothem [“digital”] correlation and biostratigraphy across the global Moscovian-

Kasimovian-Gzhelian stage boundary interval (Middle-Upper Pennsylvanian) in North America and eastern Europe." *Geology* 35, no. 7 (2007): 607-610.

Isbell, John L., Molly F. Miller, Keri L. Wolfe, Paul A. Lenaker, M. A. Chan, and A. W. Archer. "Timing of late Paleozoic glaciation in Gondwana: was glaciation responsible for the development of Northern Hemisphere cyclothems?" *Special Papers-Geological Society of America* (2003): 5-24.

Isbell, John L., Paul A. Lenaker, Rosemary A. Askin, Molly F. Miller, and Loren E. Babcock. "Reevaluation of the timing and extent of late Paleozoic glaciation in Gondwana: Role of the Transantarctic Mountains." *Geology* 31, no. 11 (2003): 977-980.

Isbell, John L., Margaret L. Fraiser, and Lindsey C. Henry. "Examining the complexity of environmental change during the late Paleozoic and early Mesozoic." *Palaios* 23, no. 5 (2008): 267-269.

Johnson, Kenneth S. "Geologic evolution of the Anadarko Basin." *Oklahoma Geological Survey Circular* 90, no. 10 (1989).

Johnson, Kenneth S., and Rosemary L. Croy, eds. “Stratiform Copper Deposits of the Midcontinent Region: A Symposium.” *Oklahoma Geological Survey, Circular 77* (1976): 99pp.

Johnson, Kenneth S. "Dissolution of salt on the east flank of the Permian Basin in the southwestern USA." In *Developments in Water Science*, vol. 16, pp. 75-93. Elsevier, 1982.

Johnson, Kenneth S. "Standard outcrop section of the Blaine Formation and associated strata in southwestern Oklahoma." *Oklahoma Geology Notes* 50, no. 5 (1990): 144-168.

Johnson, Kenneth S. "Permian Blaine and San Andres Formations of western Oklahoma and Palo Duro Basin of Texas: their correlation and evaporite karst." *Oklahoma Geological Survey, Circular* 113 (2021): 247-277.

Jones, Timothy P., and Nicholas P. Rowe, eds. "Fossil Plants and Spores: modern techniques." Geological Society of London, 1999.

King, James E., Walter E. Klippel, and Rose Duffield. "Pollen preservation and archaeology in eastern North America." *American Antiquity* (1975): 180-190.

Kluth, Charles F., and Peter J. Coney. "Plate tectonics of the ancestral Rocky Mountains." *Geology* 9, no. 1 (1981): 10-15.

Lakin, J. A., J. E. A. Marshall, I. Troth, and I. C. Harding. "Greenhouse to icehouse: a biostratigraphic review of latest Devonian–Mississippian glaciations and their global effects." *Geological Society, London, Special Publications* 423, no. 1 (2016): 439-464.

LaPoint, Dennis J. "Possible source areas for sandstone copper deposits in northern New Mexico." In *Guidebook to Ghost Ranch (central-northern New Mexico): New Mexico Geological Society, 25th Field Conference*, pp. 305-308. 1974.

Lindström, Sofie, Stephen McLoughlin, and Andrew N. Drinnan. "Intraspecific variation of taeniate bisaccate pollen within Permian glossopterid sporangia, from the Prince Charles Mountains, Antarctica." *International Journal of Plant Sciences* 158, no. 5 (1997): 673-684.

Looy, Cindy V., Hans Kerp, Ivo Duijnstee, and William A. DiMichele. "The late Paleozoic ecological-evolutionary laboratory, a land-plant fossil record perspective." *The Sedimentary Record* 12, no. 4 (2014): 4-18.

Looy, Cindy V., and Carol L. Hotton. "Spatiotemporal relationships among Late Pennsylvanian plant assemblages: palynological evidence from the Markley Formation, West Texas, USA." *Review of Palaeobotany and Palynology* 211 (2014): 10-27.

Lupia, Richard, and John L. Armitage. "Late Pennsylvanian–Early Permian vegetational transition in Oklahoma: palynological record." *International Journal of Coal Geology* 119 (2013): 165-176.

Montañez, Isabel P., Neil J. Tabor, Deb Niemeier, William A. DiMichele, Tracy D. Frank, Christopher R. Fielding, John L. Isbell, Lauren P. Birgenheier, and Michael C. Rygel. "CO_2-forced climate and vegetation instability during Late Paleozoic deglaciation." *Science* 315, no. 5808 (2007): 87-91.

Montañez, Isabel P., and Christopher J. Poulsen. "The Late Paleozoic ice age: an evolving paradigm." *Annual Review of Earth and Planetary Sciences* 41 (2013): 629-656.

Morgan, William E. "Palynology of a portion of the El Reno group (Permian) southwest Oklahoma." PhD diss., The University of Oklahoma, 1967.

Parrish, Judith Totman. "Climate of the supercontinent Pangea." *The Journal of Geology* 101, no. 2 (1993): 215-233.

Parrish, Judith Totman. "Geologic evidence of Permian climate." In *The Permian of Northern Pangea*, pp. 53-61. Springer, Berlin, Heidelberg, 1995.

Peppers, Russel A. "Palynology of the Lost Branch Formation of Kansas—new insights on the major floral transition at the Middle-Upper Pennsylvanian boundary." *Review of Palaeobotany and Palynology* 98, no. 3-4 (1997): 223-246.

Pfefferkorn, Hermann W., and Margaret C. Thomson. "Changes in dominance patterns in Upper Carboniferous plant-fossil assemblages." *Geology* 10, no. 12 (1982): 641-644.

Pfefferkorn, Hermann W., Robert A. Gastaldo, William A. DiMichele, and Tom L. Phillips. "Pennsylvanian tropical floras from the United States as a record of changing climate." *Resolving the Late Paleozoic Ice Age in time and space. Geol Soc Am Spec Pap* 441 (2008): 305-316.

Phillips, Thomas L., Matthew J. Avcin, and Dwain Berggren. "Fossil peat of the Illinois Basin: a guide to the study of coal balls of Pennsylvanian age." *Geoscience Education 11* (1976).

Raymond, Charles. "Shear margins in glaciers and ice sheets." *Journal of Glaciology* 42, no. 140 (1996): 90-102.

Ripley, E. M., Michael W. Lambert, and Pieter Berendsen. "Mineralogy and paragenesis of red-bed copper mineralization in the Lower Permian of South central Kansas." *Economic Geology* 75, no. 5 (1980): 722-729.

Saltzman, Matthew R. "Late Paleozoic ice age: oceanic gateway or pCO_2?" *Geology* 31, no. 2 (2003): 151-154.

Scotese, Christopher R., and R. P. Langford. "Pangea and the paleogeography of the Permian." In *The Permian of Northern Pangea*, pp. 3-19. Springer, Berlin, Heidelberg, 1995.

Scotese, Christopher R., R. Van der Voo, S. F. Barrett, and John David Lawson. "Silurian and Devonian base maps." *Philosophical Transactions of the Royal Society of London. B, Biological Sciences* 309, no. 1138 (1985): 57-77.

Smith, Gary E. "Depositional systems, San Angelo Formation (Permian), north Texas--facies control of red-bed copper mineralization." *Virtual Landscapes of Texas* (1974).

Soreghan, Gerilyn S., Michael J. Soreghan, and Nicholas G. Heavens. "Explosive volcanism as a key driver of the late Paleozoic ice age." *Geology* 47, no. 7 (2019): 600-604.

Stampfli, G. M., C. Hochard, C. Vérard, and C. Wilhem, “The formation of Pangaea.” Tectonophysics 593 (2013): 1-19.

Stephenson, Michael H. "Permian palynostratigraphy: a global overview." *Geological Society, London, Special Publications* 450, no. 1 (2018): 321-347.

Sun, Yu-Zhuang, and Wilhem Püttmann. "The role of organic matter during copper enrichment in Kupferschiefer from the Sangerhausen basin, Germany." *Organic Geochemistry* 31, no. 11 (2000): 1143-1161.

Sweet, Alison C., Gerilyn S. Soreghan, Dustin E. Sweet, Michael J. Soreghan, and Andrew S. Madden. "Permian dust in Oklahoma: source and origin for middle Permian (Flowerpot-Blaine) redbeds in western tropical Pangaea." *Sedimentary Geology* 284 (2013): 181-196.

Traverse, Alfred. Paleopalynology: Winchester, Massachusetts. 1988.

Traverse, Alfred. Paleopalynology, 2nd Ed.: Springer Science & Business Media, 2007.

Vázquez, María Soledad, and Silvia N. Césari. "The Permian palynological *Lueckisporites-Weylandites* biozone in the San Rafael block and its correlation in western Gondwana." *Journal of South American Earth Sciences* 76 (2017): 165-181.

Visscher, Henk, Henk Brinkhuis, David L. Dilcher, William C. Elsik, Yoram Eshet, Cindy V. Looy, Michael R. Rampino, and Alfred Traverse. "The terminal Paleozoic fungal event: evidence of terrestrial ecosystem destabilization and collapse." *Proceedings of the National Academy of Sciences* 93, no. 5 (1996): 2155-2158.

Wicander, Reed, and James S. Monroe. *Historical Geology*. Cengage Learning, 2015.

Wilson, Leonard R.. “A Permian hystrichosphaerid from Oklahoma.” *Oklahoma Geology Notes*, *20* (1960): 170.

Wilson, Leonard R. “A Permian fungus spore type from the Flowerpot Formation of Oklahoma.” *Oklahoma Geology Notes*, *22* (1962): 91-96.

Wilson, Leonard R. "Permian plant microfossils from the Flowerpot Formation, Oklahoma.” *Oklahoma Geological Survey Bulletin* 49 (1962): 5-50.

Zavialova, N. E., N. R. Meyer-Melikian, and A. V. Gomankov. "Ultrastructure of some Permian pollen grains from the Russian Platform." In *Proceedings of the IX International Palynological Congress, Houston (Texas, USA, 1996). American Association of Stratigraphic Palynologists Foundation*, pp. 99-114. 2001.

Ziegler, Alfred M., Peter McA. Rees, and Serge V. Naugolnykh. "The Early Permian floras of Prince Edward Island, Canada: differentiating global from local effects of climate change." *Canadian Journal of Earth Sciences* 39, no. 2 (2002): 223-238.

TABLE 1

Taxonomic diversity of taxa identified in each sample that was quantitatively counted, including those outside of the 300-grain count by scanning the whole slide after reaching 300.

Specimen \ Slide #	2255	2254	2253	2251	2250	2248	2247	2241	2235	2227
Trilete spore type 1				1	1	1		1		1
Trilete spore type 2					1					
Trilete spore type 3				1	1		1	1	1	
Calamospora sp.								1		
Trilete spore type 5				1		1	1	1	1	
Trilete spore type 6				1	1					
Trilete spore type 7				1		1		1	1	
Trilete spore type 8									1	
Trilete spore type 9						1		1		
Trilete spore type 10							1		1	
Trilete spore type 11	1			1	1	1	1	1	1	
Trilete spore type 12								1		
Trilete spore type 13										1
Trilete spore type 14						1				
Trilete spore type 15							1			
Trilete spore type 16									1	
Trilete spore type 17					1					
Laevigatosporites sp.	1	1	1	1	1	1	1	1	1	1
Protohaploxypinus? sp. 1			1		1	1	1	1	1	1
Protohaploxypinus? sp. 2			*identified only from a survey sample*							
Protohaploxypinus? sp. 3								1		1
Alisporites sp. 1	1	1	1	1	1	1	1	1	1	1
Alisporites sp. 2					1	1				
Alisporites sp. 3				1	1	1			1	1
Limitisporites sp. 1			*identified only from a survey sample*							
Limitisporites sp. 2							1	1		
Bisaccate pollen type 1					1				1	
Bisaccate pollen type 2			*identified only from a survey sample*							
Bisaccate pollen type 3			*identified only from a survey sample*							
Bisaccate pollen type 4				1		1	1			
Bisaccate pollen type 5			*identified only from a survey sample*							
Bisaccate pollen type 6			*identified only from a survey sample*							
Bisaccate pollen type 7									1	
Strotersporites sp.	1		1	1	1	1	1	1	1	1
Bisaccate pollen type 9				1	1	1	1	1	1	1
Bisaccate pollen type 10				1	1	1	1	1	1	1
Bisaccate pollen type 11			*identified only from a survey sample*							
Lueckisporites virkkiae	1	1	1	1	1	1	1	1	1	1
Hamiapollenites perisporites						1			1	
Vittatina costabilis	1			1	1	1	1	1	1	1
Vittatina lata	1		1	1	1	1	1	1	1	1
Potonieisporites spp.	1			1	1	1		1	1	
Psophosphaera? sp.	1	1	1	1	1	1	1	1	1	1
Brachysporisporites? sp.		1								
Paleomycites? sp.		1	1							
Fungal spore type 3		1	1							

TABLE 2

Abundance of grains belonging to each taxon identified within the 300-grain quantitative count. If fewer than 300 grains were observed on slide, all encountered grains are reported.

Specimen \ Slide #	2255	2254	2253	2251	2250	2248	2247	2241	2235	2227
Trilete spores	1	0	0	6	2	4	2	5	3	1
Laevigatosporites sp.	1	7	3	2	2	1	3	3	4	2
Protohaploxypinus? sp. 1	0	0	1	0	5	5	3	1	2	3
Protohaploxypinus? sp. 3	0	0	0	0	0	0	0	1	0	3
Alisporites sp. 1	9	2	1	18	22	13	11	6	6	6
Alisporites sp. 2	0	0	0	0	1	1	0	0	0	0
Alisporites sp. 3	0	0	0	1	1	3	0	0	2	1
Limitisporites sp. 2	0	0	0	0	0	0	1	2	0	0
Bisaccate pollen type 1	0	0	0	0	2	0	0	0	1	0
Bisaccate pollen type 4	0	0	0	1	0	1	2	0	0	0
Bisaccate pollen type 7	0	0	0	0	0	0	0	0	1	0
Strotersporites sp.	1	0	1	20	21	13	18	15	17	3
Bisaccate pollen type 9	0	0	0	12	11	7	5	2	2	1
Bisaccate pollen type 10	0	0	0	3	2	1	3	3	4	2
Lueckisporites virkkiae	50	13	22	226	215	238	241	244	238	50
Hamiapollenites perisporites	0	0	0	0	0	2	0	0	1	0
Vittatina costabilis	1	0	0	2	6	2	1	3	3	2
Vittatina lata	2	0	4	4	5	4	7	9	10	1
Potonieisporites spp.	1	0	0	2	1	2	0	1	3	0
Psophosphaera? sp.	1	2	1	3	4	3	3	5	3	7
Brachysporisporites? sp.	0	100	0	0	0	0	0	0	0	0
Paleomycites? sp.	0	18	26	0	0	0	0	0	0	0
Fungal spore type 3	0	3	48	0	0	0	0	0	0	0
Total Counted Specimens	67	145	107	300	300	300	300	300	300	82

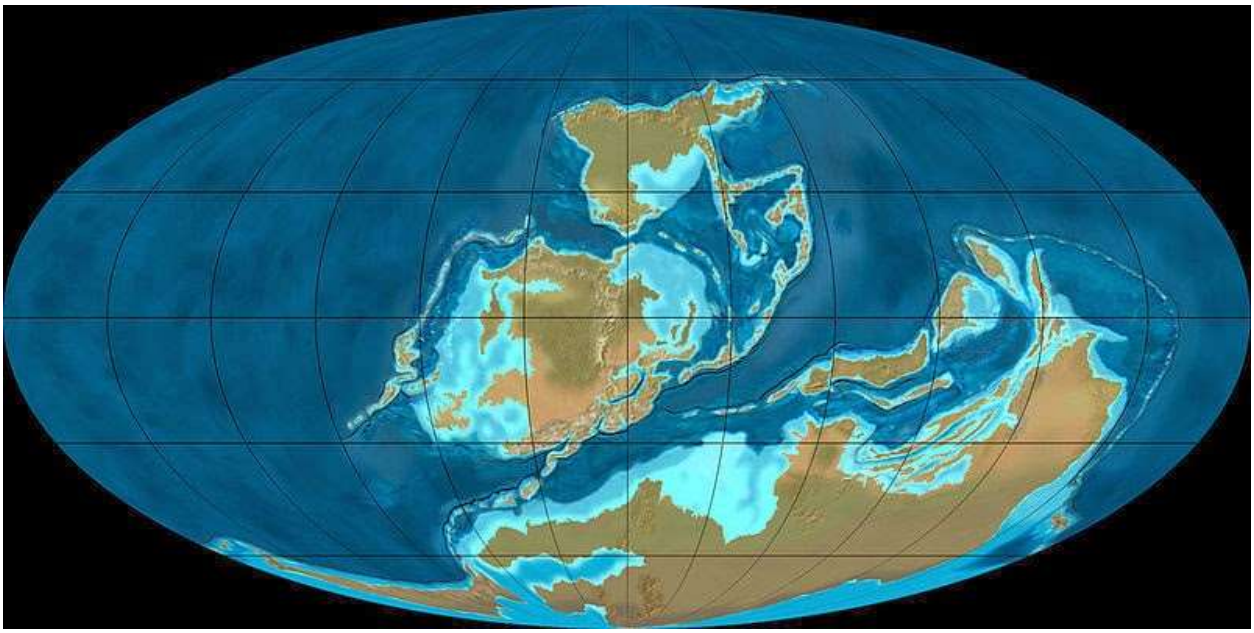

FIGURE 1. Paleogeography during Late Devonian showing Gondwana located around the southern polar region. (image from Blakely, 2014)

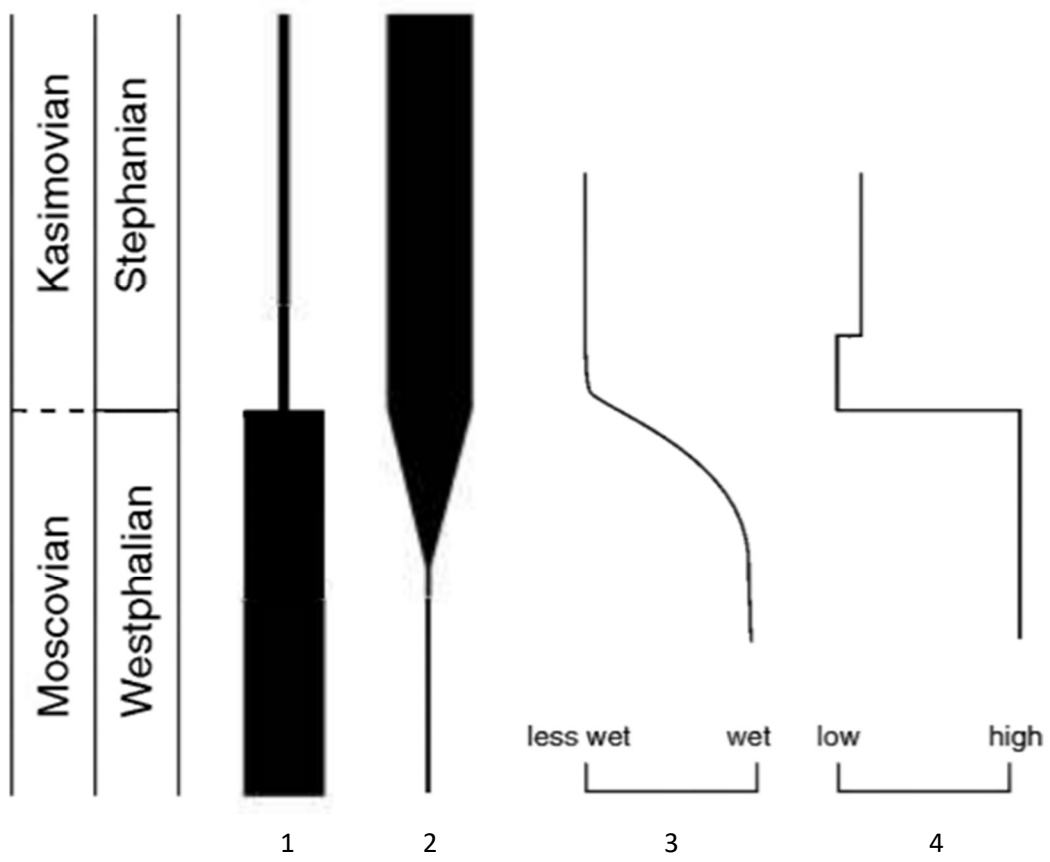

FIGURE 2. Changes in abundance of column 1) tree lycopods and column 2) tree ferns across Westphalian-Stephanian boundary (Middle and Upper Pennsylvanian boundary). Column 3) Wetness of Illinois Basin area and 4) inferred ice volume on Gondwana after Frakes et al., 1992 (modified from Pfefferkorn et al., 2008).

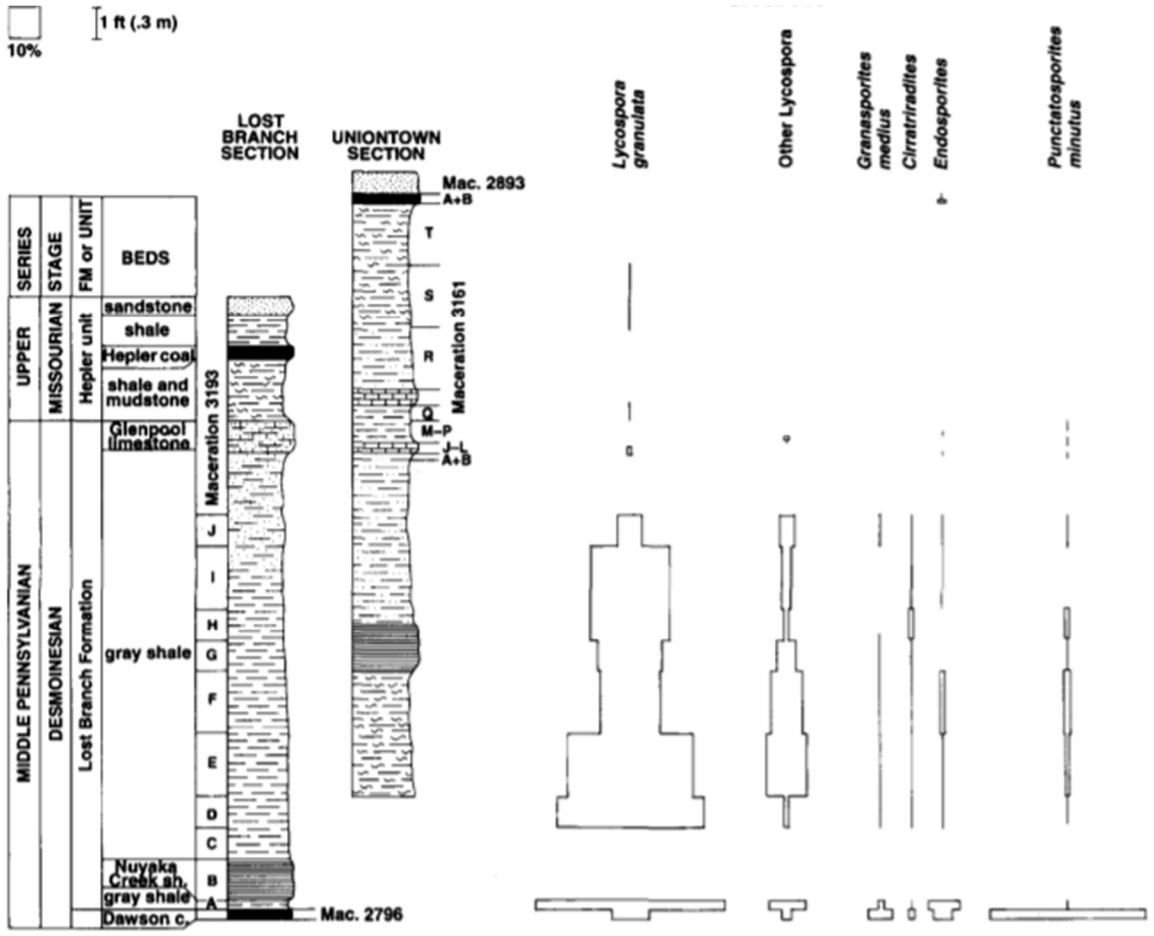

FIGURE 3. Palynological data of Lost Branch Formation showing decrease in abundance of multiple lycopod spore species across Middle to Upper Pennsylvanian boundary (Moscovian–Kasimovian) (modified from Peppers, 1997).

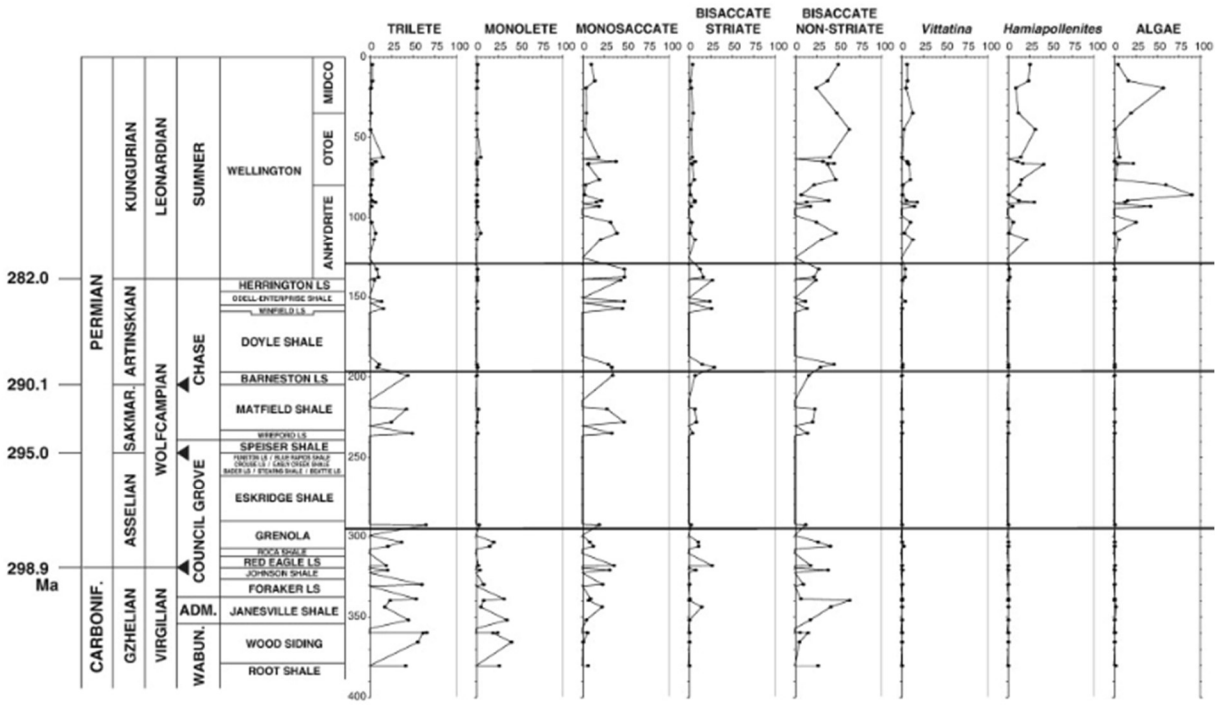

FIGURE 4. Palynological data showing the changes in spore floras from cores in north central Oklahoma representing the latest Carboniferous to the Early Permian. Note that major changes were not (locally) associated with the Pennsylvanian-Permian boundary (in Red Eagle Formation). A notable but not simultaneous transition occurs as monolete, then trilete spores diminish and seed plants, including *Vittatina* and *Hamiapollenites*, show marked increase in abundance into the Permian (modified from Lupia and Armitage, 2013).

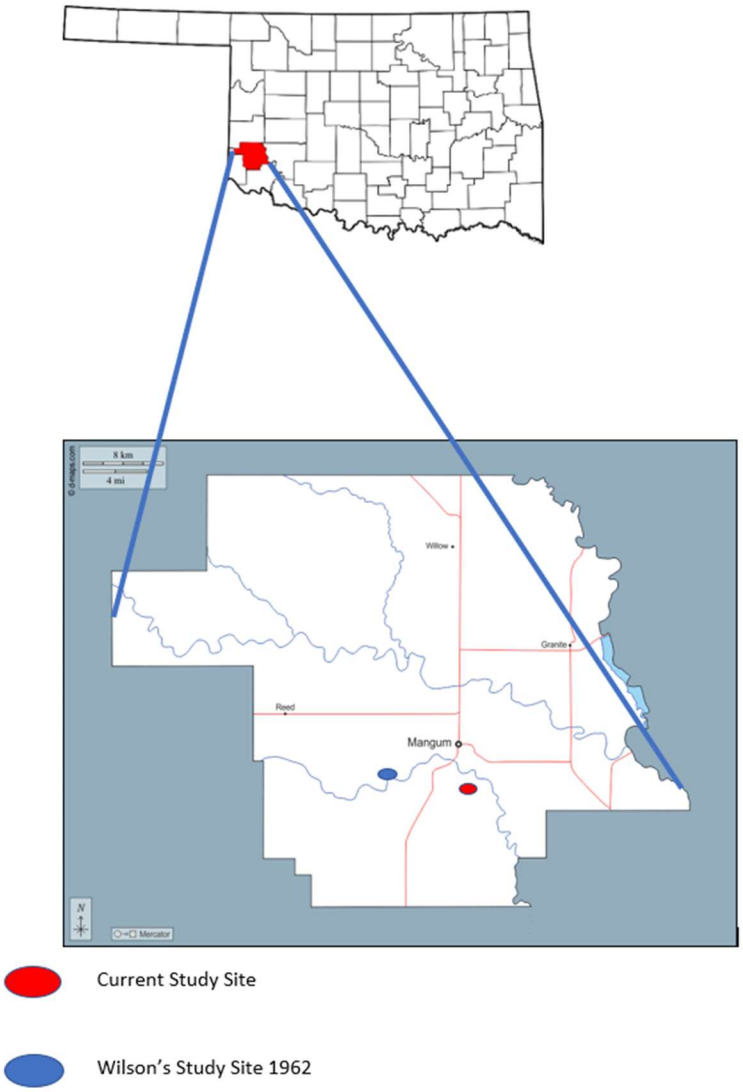

FIGURE 5. Oklahoma state and Greer County map showing current study site in relation to Wilson's (1960, 1962) study site.

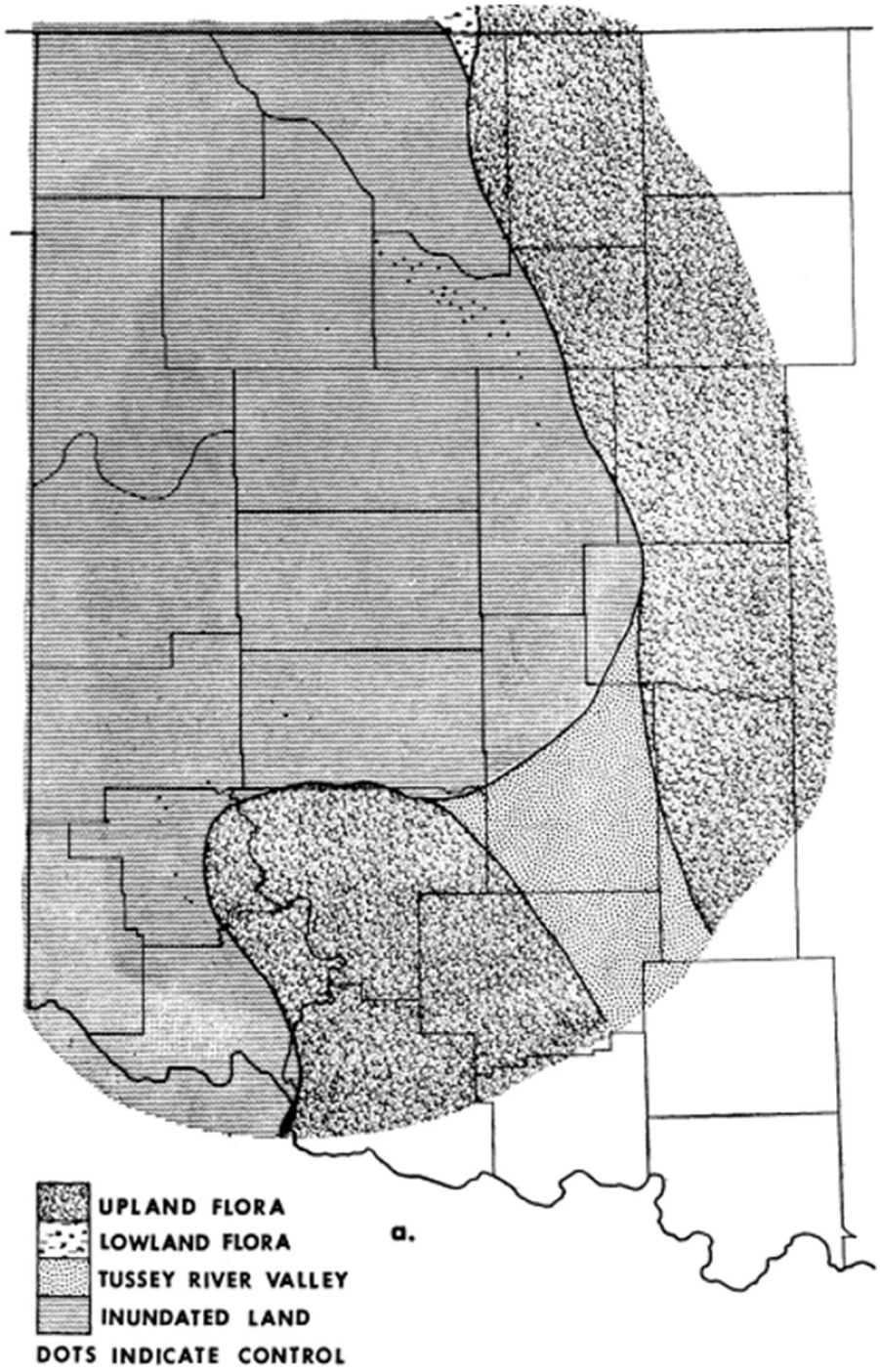

FIGURE 6. Clapham's interpretation of western Oklahoma showing transgressive interval and predominance of upland flora ("Assemblage G") in depositional basin (modified from Clapham, 1970).

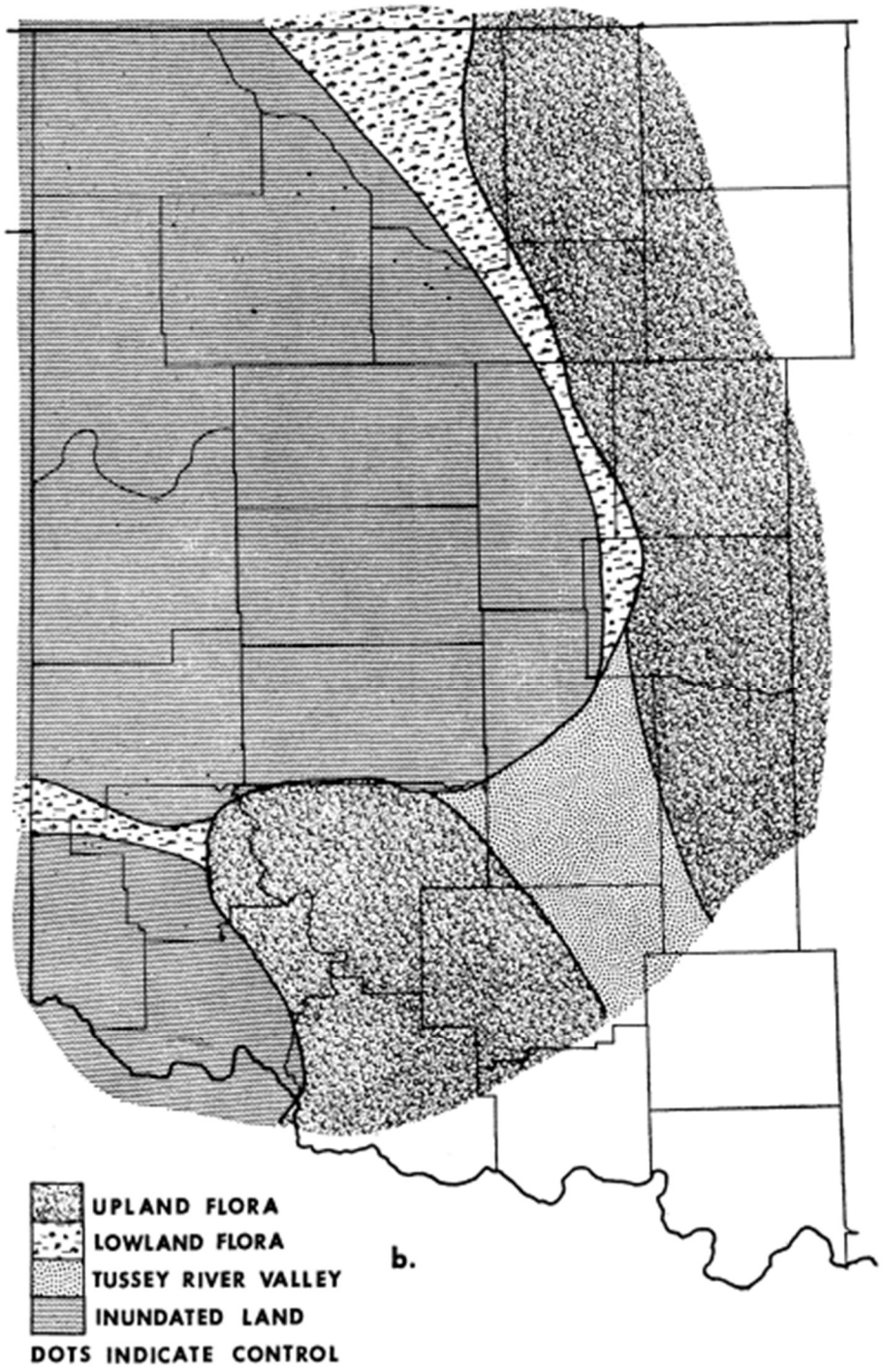

FIGURE 7. Clapham's intepretation of western Oklahoma showing regressive interval and increase in lowland flora (generating "Assemblage F") in depositional basin (modified from Clapham, 1970).

FIGURE 8. Satellite oblique view of study area looking to north (image from Google Earth). The approximate position of Bed 20 (“copper interval”) is shown by green arrow.

FIGURE 9. Ground level view of study area looking to north (photo by author). The approximate position of Bed 20 (“copper interval”) is shown by green arrow.

FIGURE 10. View showing upper portion of bed 20 (“copper interval”). A gypsiferous mudstone (bed 21) is at the top of the scale. The Kiser Gypsum (bed 24) is the thick white bed in the image. Scale bar = 50 cm (photo by author).

FIGURE 11. Close-up of bed 20 showing green flecks of copper (malachite). Scale bar = 10 cm (photo by author)

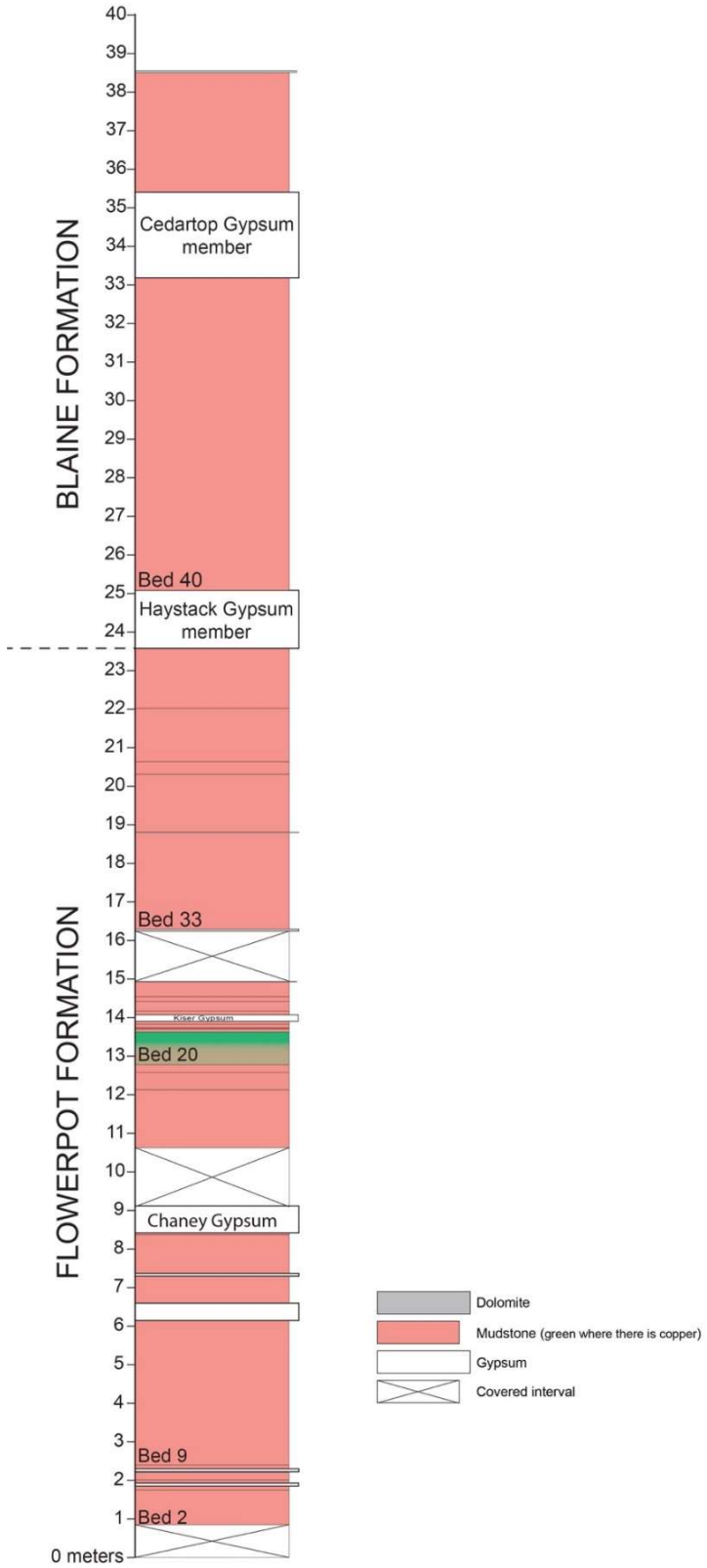

Figure 12. Measured section in study area. See text ("Materials and Methods") for description of individual beds; Bed 20 is the "copper interval" and main target of study. The Kiser Gypsum (Bed 25) is the thin gypsum at 14 m above the base of section.

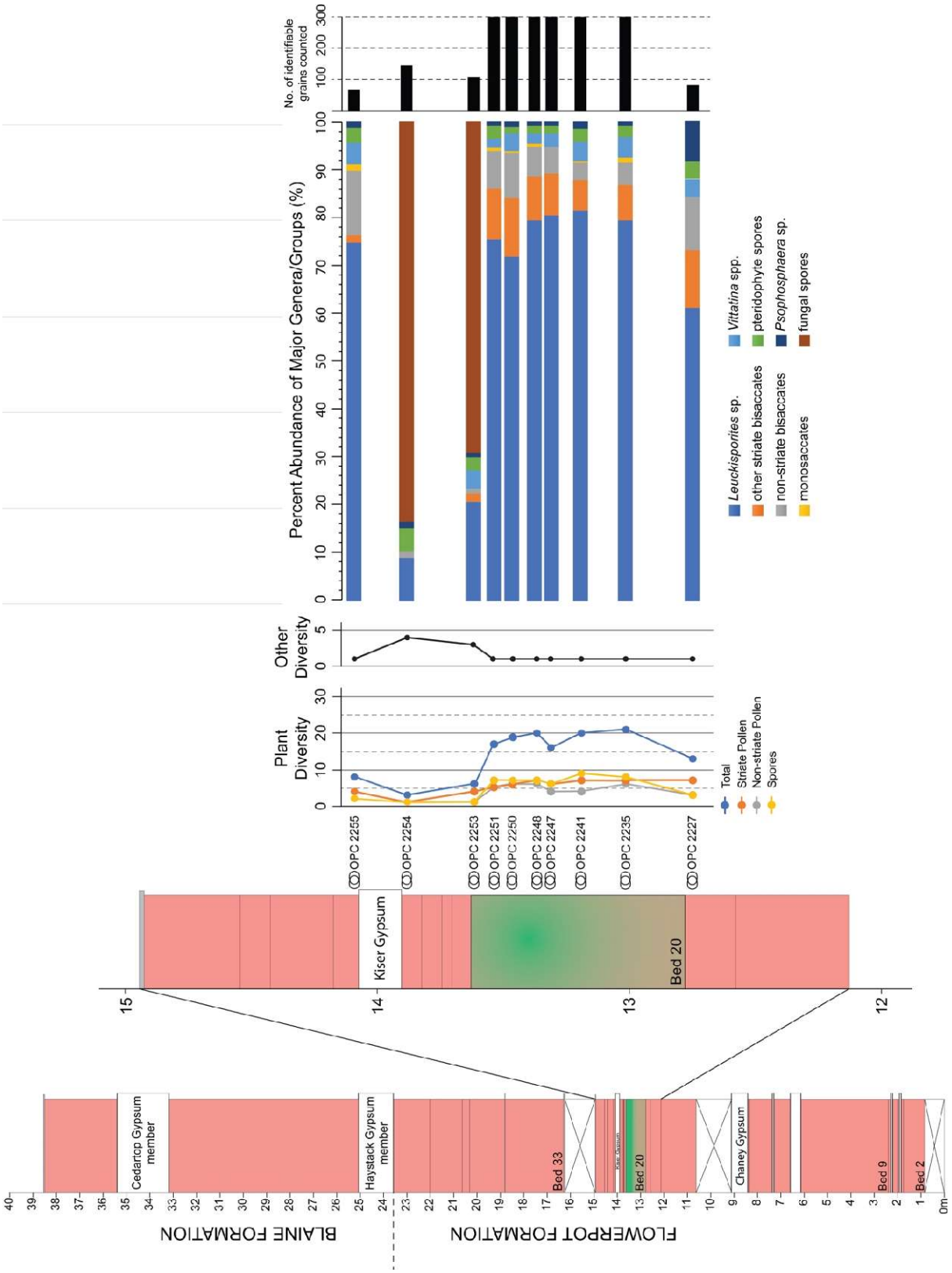

Figure 13. Summary of palynological results—species diversity, abundance of major groups, sample specimen counts—according to the position of samples in the measured section. "Other diversity" refers to fungal plus algal species.

PLATE 1

(For all images, scale bar equals 100µm)

Figure 1. Trilete spore type 1. OPC 2241_40515. Coordinates: 146.2 x 10.0.

Figure 2. Trilete spore type 2. OPC 2250_40536. Coordinates: 140.9 x 4.0.

Figure 3. Trilete spore type 3. OPC 2241_40512. Coordinates: 147.1 x 14.0.

Figure 4. *Calamospora* sp. OPC 2241_40512. Coordinates: 113.0 x 14.8.

Figure 5. Trilete spore type 5. OPC 2241_40512. Coordinates: 128.8 x 17.5.

Figure 6. Trilete spore type 6. OPC 2251_40542. Coordinates: 146.1 x 15.0.

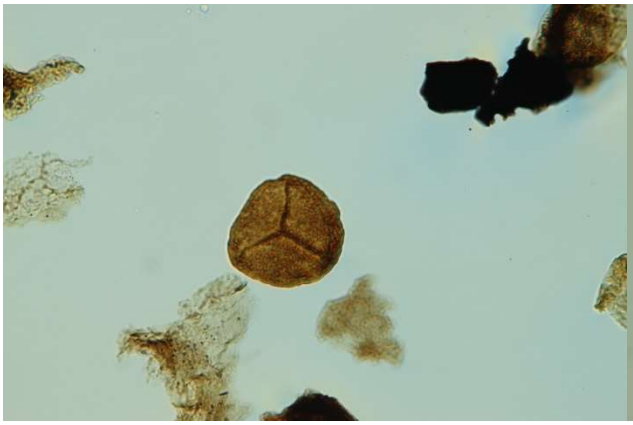

1

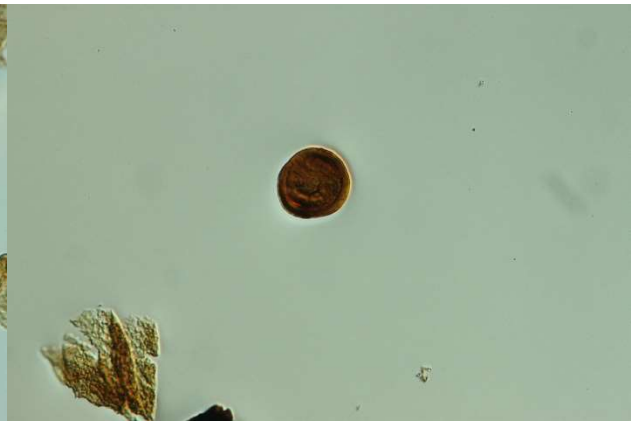

2

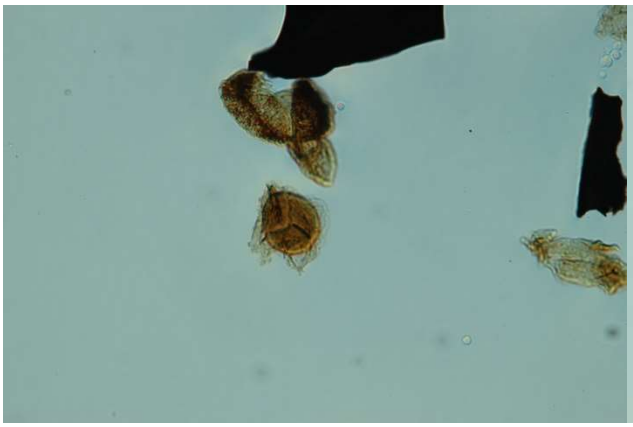

3

4

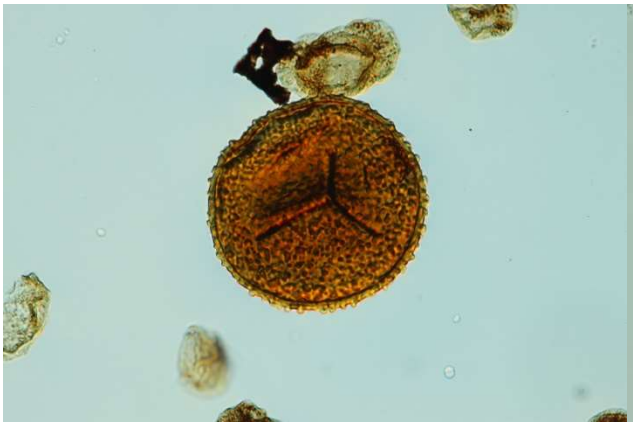

5

6

PLATE 2

(For all images, scale bar equals 100μm)

Figure 1. Trilete spore type 7. OPC 2221_31513. Coordinates: 129.6 x 7.1

Figure 2. Trilete spore type 8. OPC 2241_40513. Coordinates: 143.9 x 4.2

Figure 3. Trilete spore type 9. OPC 2223_31523. Coordinates: 122.2 x 16.9

Figure 4. Trilete spore type 10. OPC 2241_40512. Coordinates: 128.9 x 17.1

Figure 5. Trilete spore type 11. OPC 2227_40487. Coordinates: 116.5 x 8.5

Figure 6. Trilete spore type 12. OPC 2235_40498. Coordinates: 128.6 x 10.5

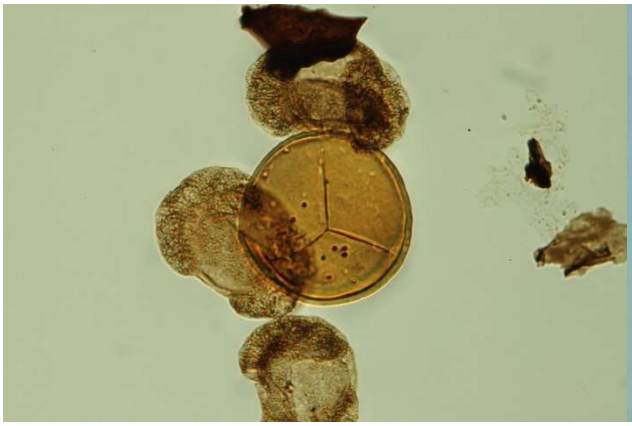

1

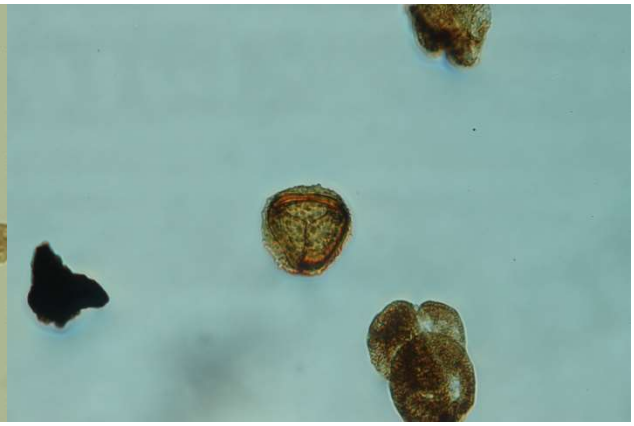

2

3

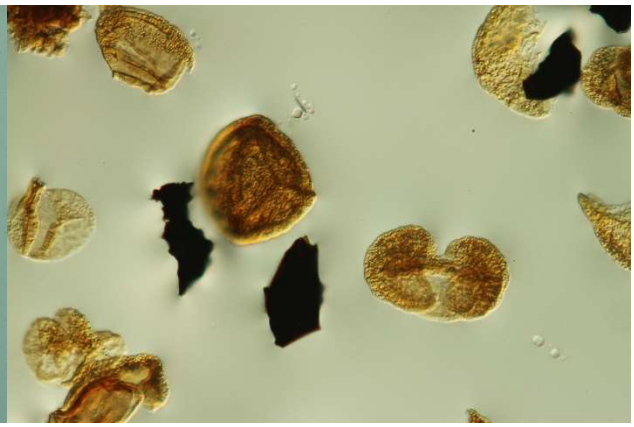

4

5

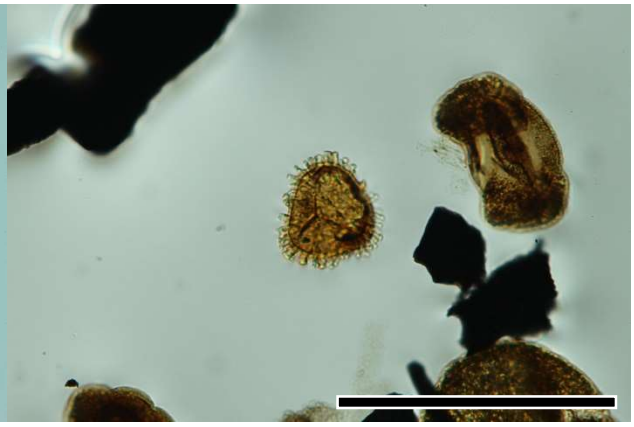

6

PLATE 3

(For all images, scale bar equals 100µm)

Figure 1. Trilete spore type 13. OPC 2250_40538. Coordinates: 132.0 x 21.0.

Figure 2. Trilete spore type 14. OPC 2221_31515. Coordinates: 141.3 x 13.9.

Figure 3. Trilete spore type 15. OPC 2221_31515. Coordinates: 128.9 x 2.4.

Figure 4. Trilete spore type 16. OPC 2248_40532. Coordinates: 119.5 x 11.5.

Figure 5. Trilete spore type 17. OPC 2247_40528. Coordinates: 118.0 x 7.5.

Figure 6. *Laevigatosporites* sp. OPC 2221_31515. Coordinates: 129.9 x 14.0.

1

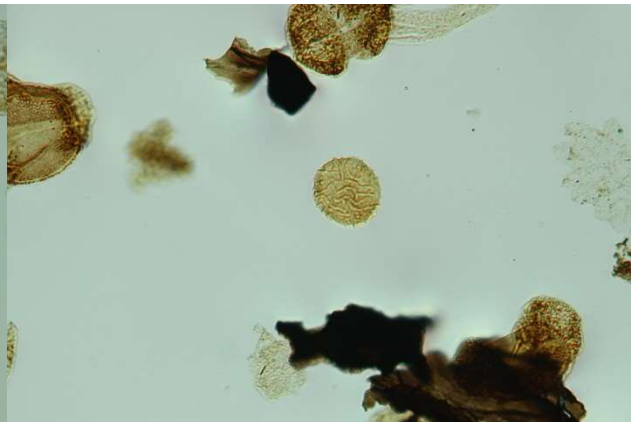

2

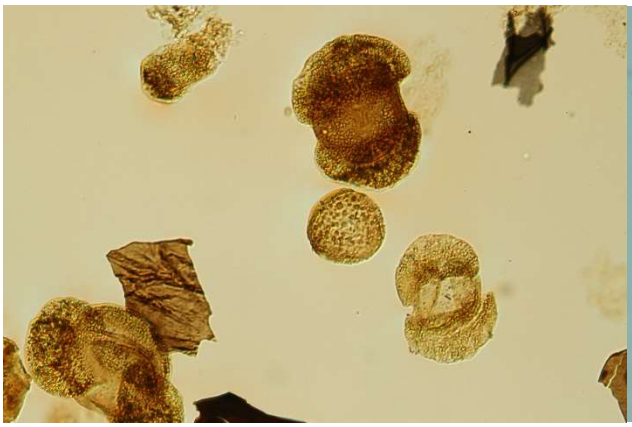

3

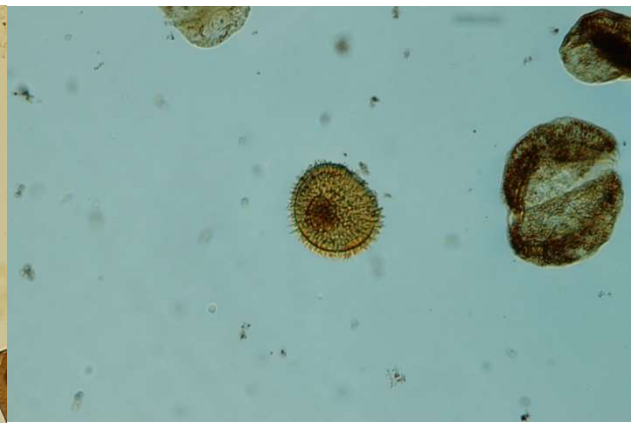

4

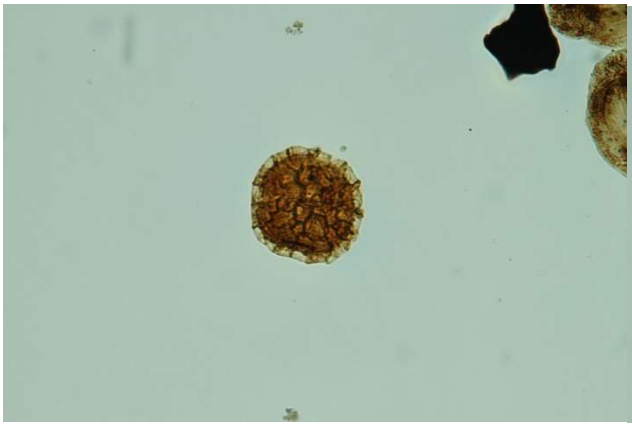

5

6

PLATE 4

(For all images, scale bar equals 100µm)

Figure 1. *Protohaploxypinus*? sp. 1. OPC 2222_31518. Coordinates: 141.3 x 9.2.

Figure 2. *Protohaploxypinus*? sp. 2. OPC 2221_31515. Coordinates: 137.4 x 21.4.

Figure 3. *Protohaploxypinus*? sp. 3. OPC 2221_31513. Coordinates: 145.9 x 17.6.

Figure 4. *Alisporites* sp. 1. OPC 2221_31516. Coordinates: 128.3 x 12.1.

Figure 5. *Alisporites* sp. 2. OPC 2221_31514. Coordinates: 126.8 x 16.1.

Figure 6. *Alisporites* sp. 3. OPC 2223_31523. Coordinates: 127.5 x 14.5.

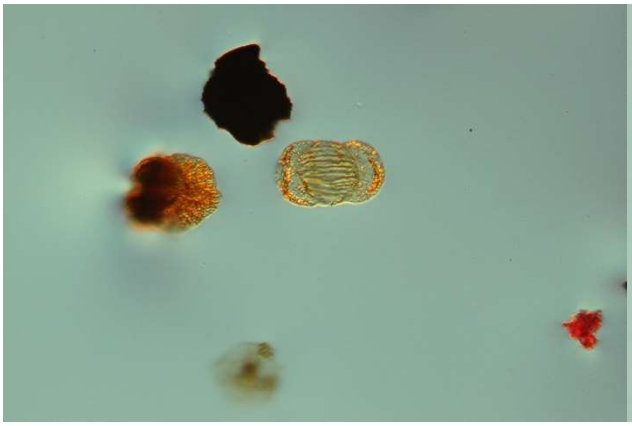

1

2

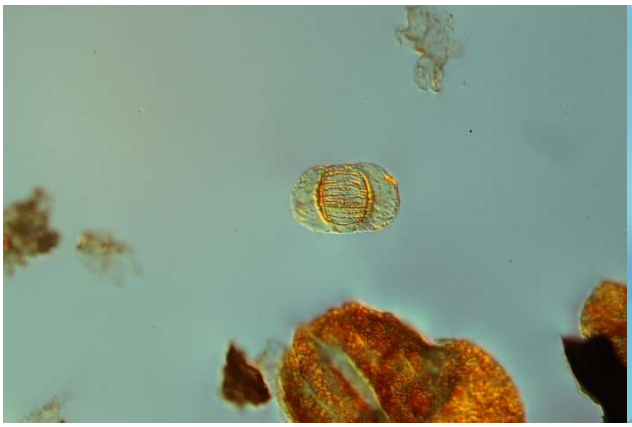

3

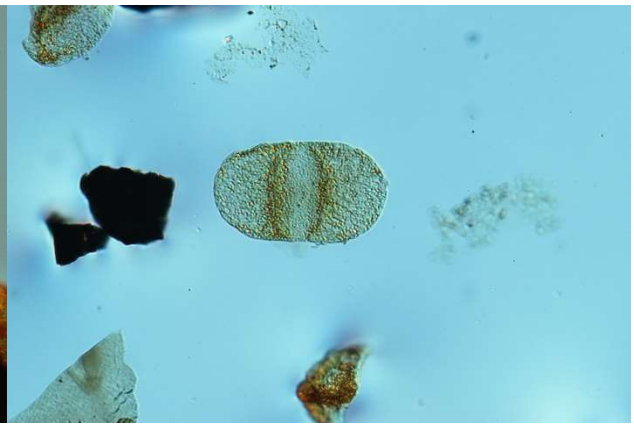

4

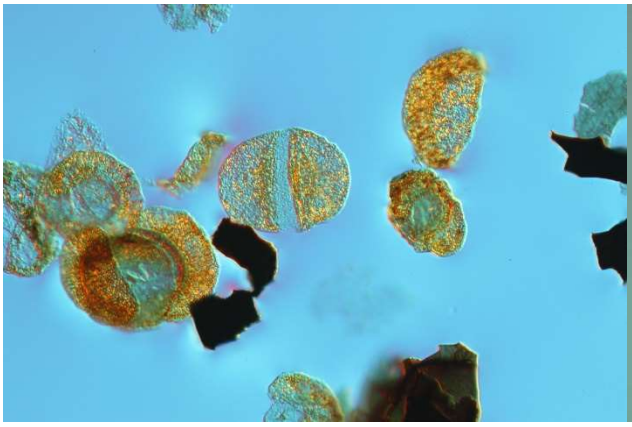

5

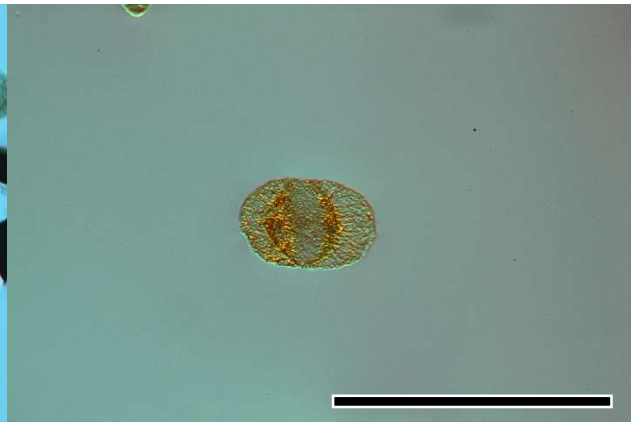

6

PLATE 5

(For all images, scale bar equals 100µm)

Figure 1. *Limitisporites* sp. 1. OPC 2221_31515. Coordinates: 136.2 x 18.9.

Figure 2. *Limitisporites* sp. 2. OPC 2222_31518. Coordinates: 136.4 x 16.2.

Figure 3. Bisaccate pollen type 1. OPC 2223_31523. Coordinates: 131.5 x 15.0.

Figure 4. Bisaccate pollen type 2. OPC 2223_31523. Coordinates: 150.5 x 18.0.

Figure 5. Bisaccate pollen type 3. OPC 2221_31515. Coordinates: 142.8 x 5.5.

Figure 6. Bisaccate pollen type 4. OPC 2221_31515. Coordinates: 117.0 x 8.4.

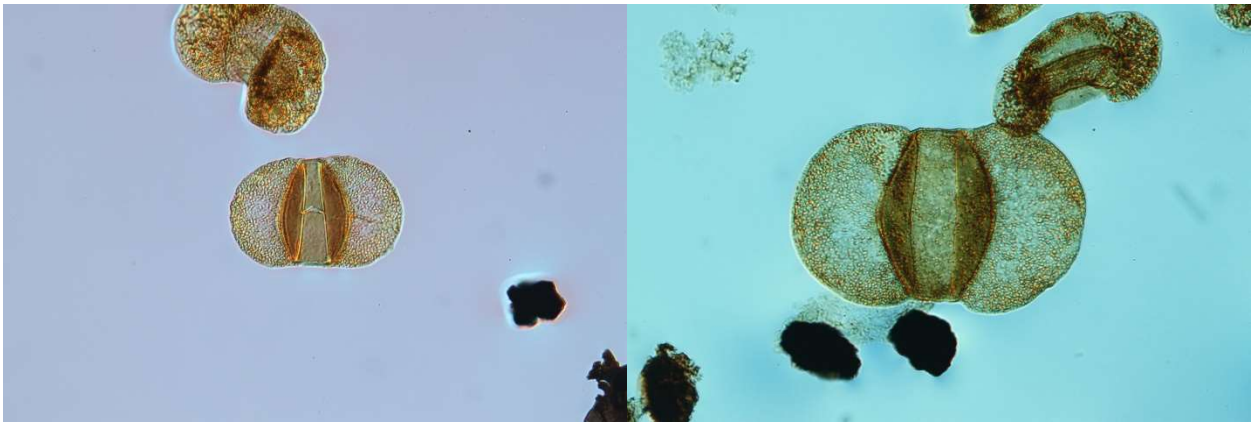

1 2

2 4

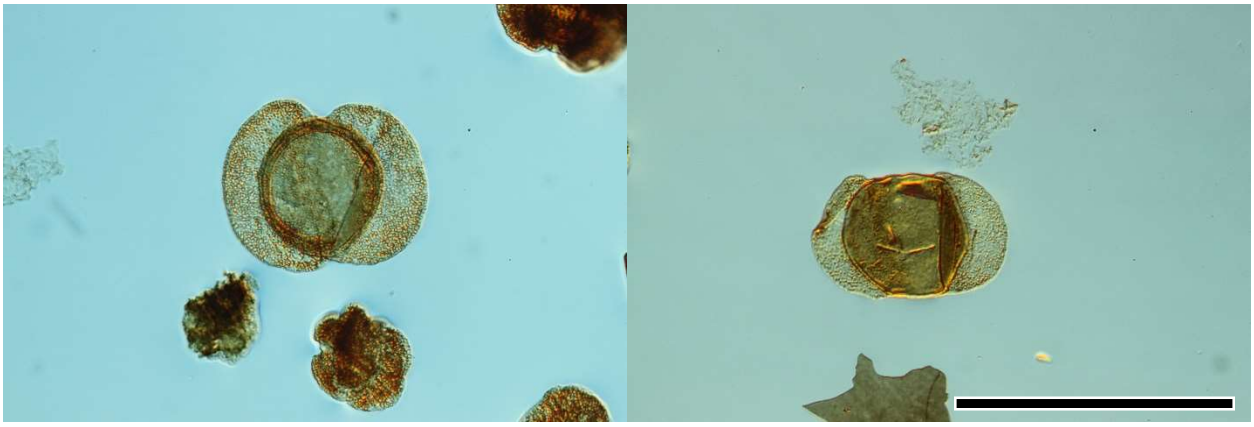

5 6

PLATE 6

(For all images, scale bar equals 100µm)

Figure 1. Bisaccate pollen type 5. OPC 2223_31523. Coordinates: 147.1 x 14.0.

Figure 2. Bisaccate pollen type 6. OPC 2223_31524. Coordinates: 126.4 x 12.2.

Figure 3. Bisaccate pollen type 7. OPC 2222_31519. Coordinates: 119.1 x 21.1.

Figure 4. *Strotersporites* sp. OPC 2223_31523. Coordinates: 138.4 x 7.5.

Figure 5. Bisaccate pollen type 9. OPC 2221_31514. Coordinates: 122.3 x 15.0.

Figure 6. Bisaccate pollen type 10. OPC 2221_31513. Coordinates: 126.1 x 21.5.

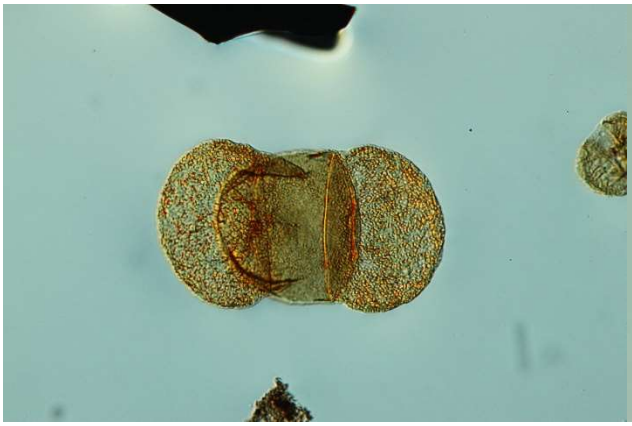

1

2

3

4

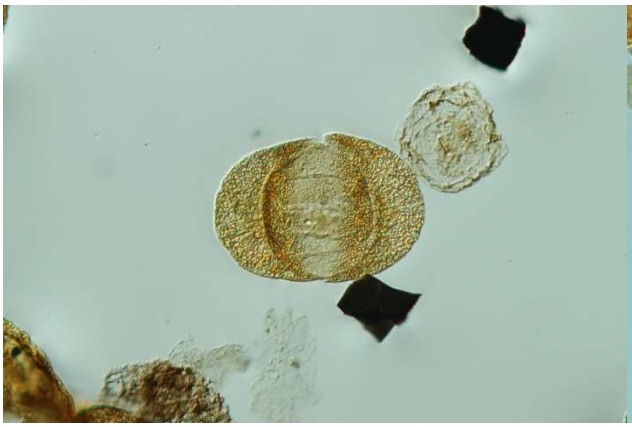

5

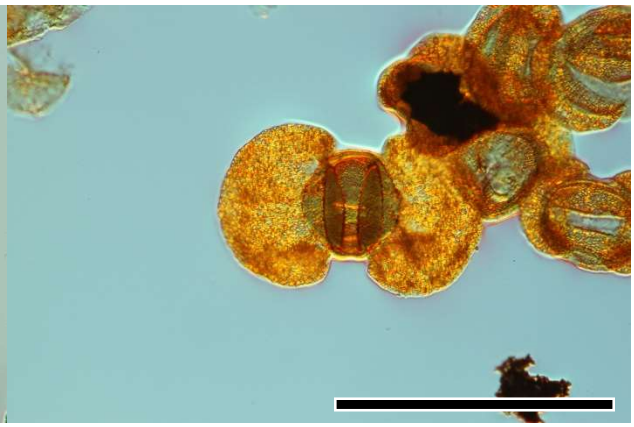

6

PLATE 7

(For all images, scale bar equals 100µm)

Figure 1. Bisaccate pollen type 11. OPC 2223_31524. Coordinates: 142.5 x 21.1.

Figure 2. *Lueckisporites virkkiae*. OPC 2221_31514. Coordinates: 148.7 x 11.8.

Figure 3. *Lueckisporites virkkiae*. OPC 2223_31523. Coordinates: 136.1 x 18.0.

Figure 4. *Lueckisporites virkkiae*. OPC 2221_31515. Coordinates: 141.4 x 3.9.

Figure 5. *Lueckisporites virkkiae*. OPC 2221_31513. Coordinates: 113.3 x 20.2 (high focus).

Figure 6. *Lueckisporites virkkiae*. OPC 2221_31513. Coordinates: 113.3 x 20.2 (low focus).

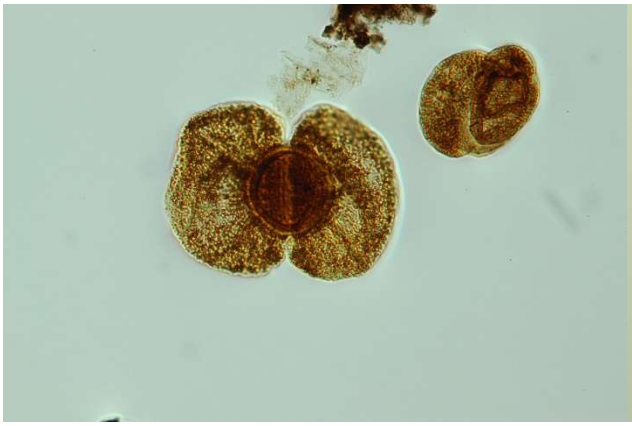

1

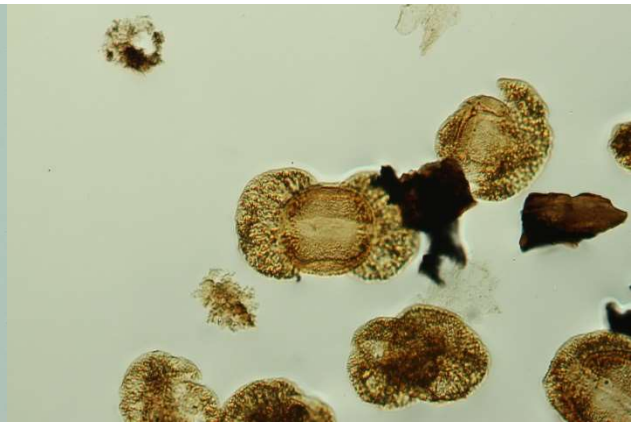

2

3

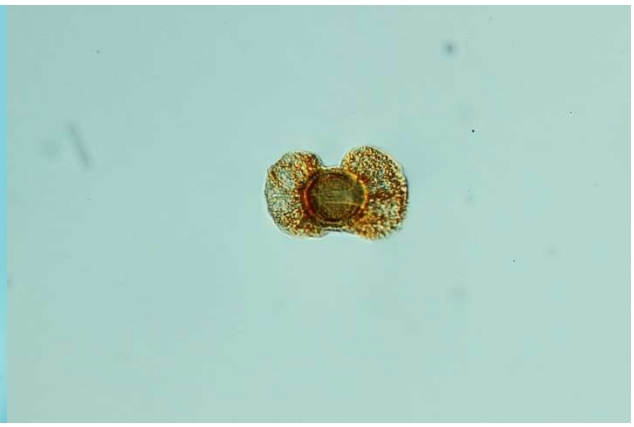

4

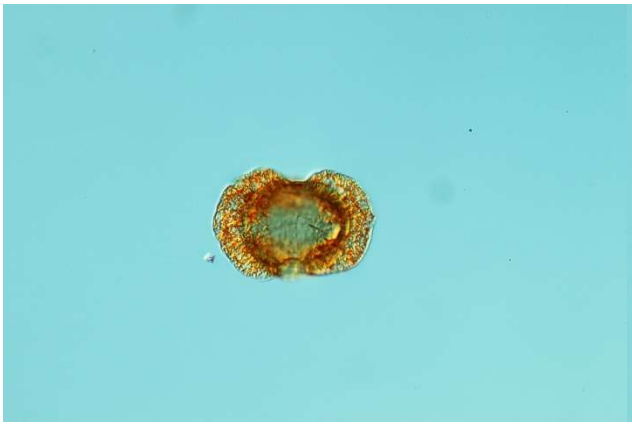

5

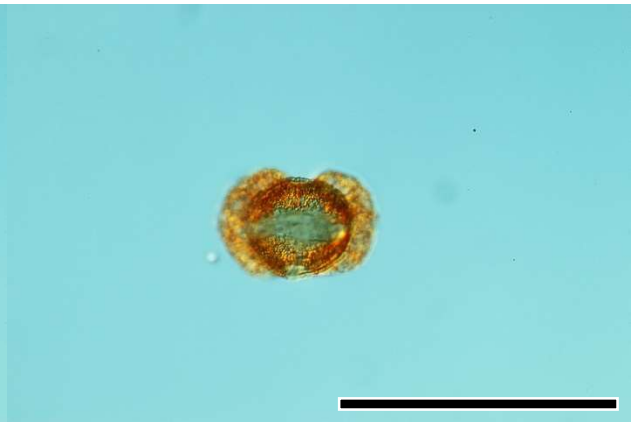

6

PLATE 8

(For all images, scale bar equals 100µm)

Figure 1. *Hamiapollenites perisporites*. OPC 2223_31523. Coordinates: 119.9 x 7.0.

Figure 2. *Hamiapollenites perisporites*. OPC 2221_31513. Coordinates: 135.1 x 17.0.

Figure 3. *Vittatina costabilis*. OPC 2221_31513. Coordinates: 132.8 x 9.0 .

Figure 4. *Vittatina lata*. OPC 2222_31519. Coordinates: 134.5 x 13.5.

Figure 5. *Potonieisporites* sp. 1. OPC 2223_31523. Coordinates 136.5 x 11.9.

Figure 6. *Potonieisporites* sp. 2. OPC 2223_31524. Coordinates 121.4 x 9.5.

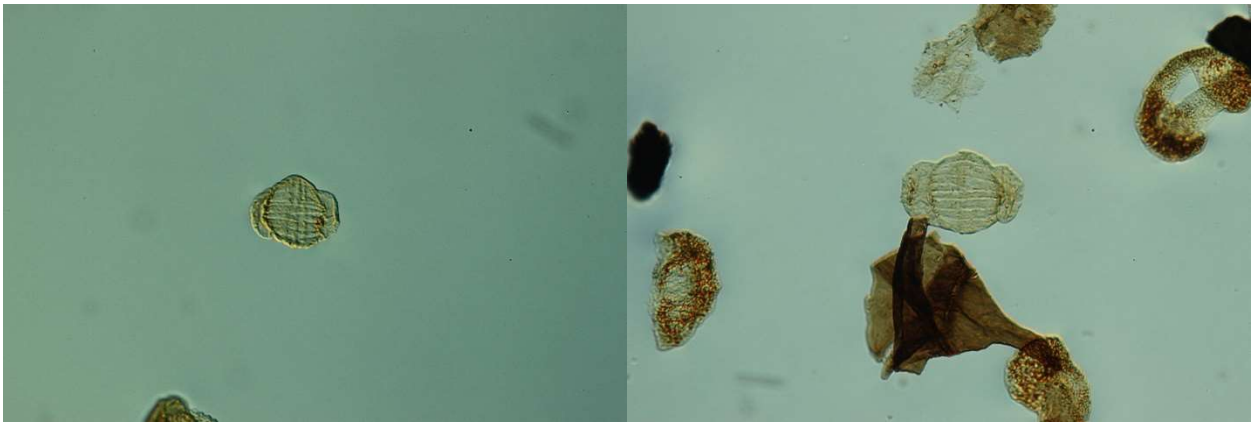

1 2

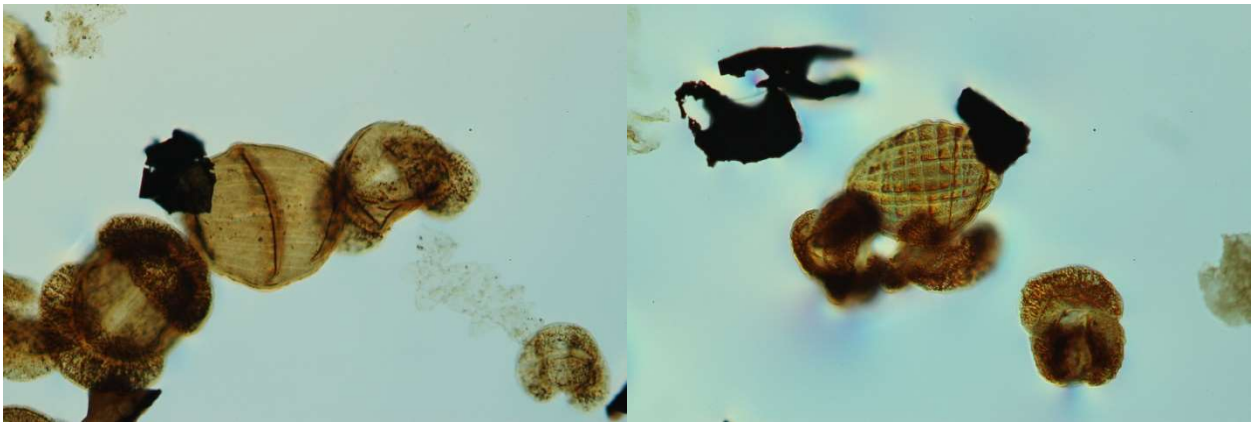

3 4

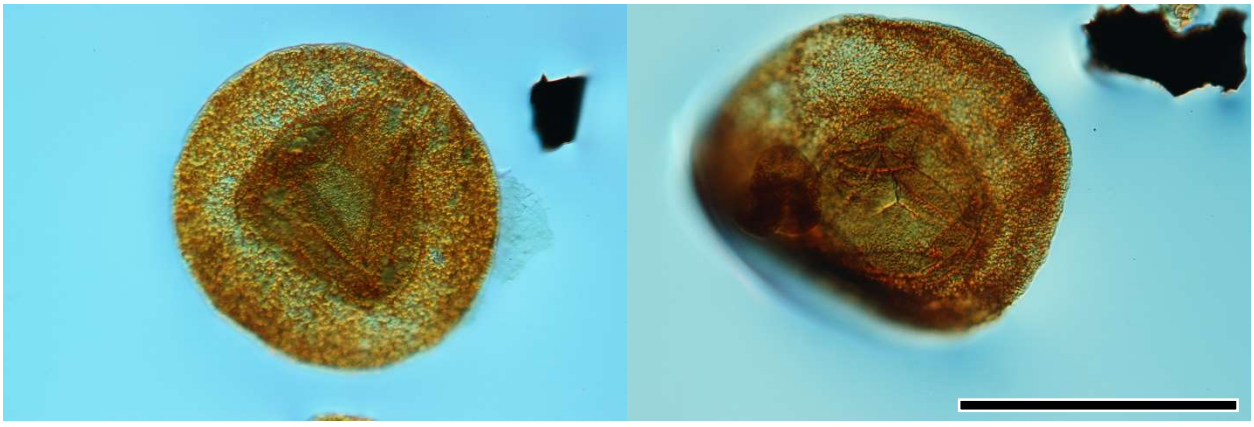

5 6

PLATE 9

(For all images, scale bar equals 100µm)

Figure 1. *Psophosphaera*? sp. OPC 2254_40548. Coordinates 140.1 x 8.1.

Figure 2. *Brachysporisporites*? sp. OPC 2254_40548. Coordinates 144.0 x 18.0.

Figure 3. *Brachysporisporites*? sp. OPC 2254_40548. Coordinates 141.0 x 17.0.

Figure 4. *Paleomycites*? sp. OPC 2254_40548. Coordinates 136.1 x 5.8.

Figure 5. *Paleomycites*? sp. OPC 2254_40548. Coordinates 125.1 x 8.2.

Figure 6. Fungal spore type 3. OPC 2253_40546. Coordinates 137.0 x 17.0.

1

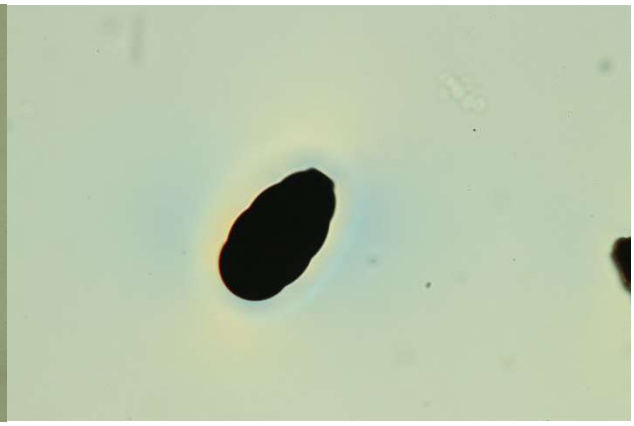

2

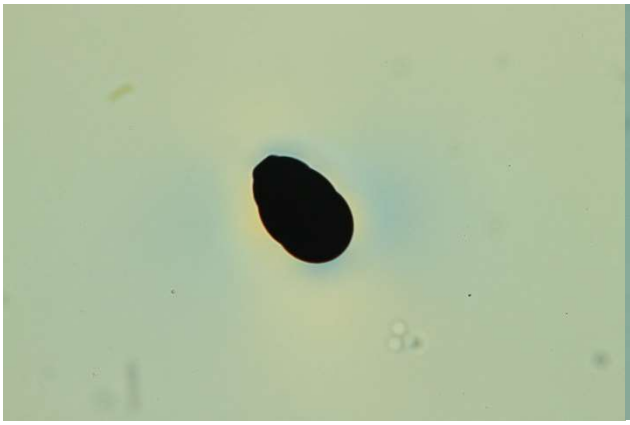

3

4

5

6